Measuring the hidden aspects of solar magnetism

J.O. Stenflo
Institute of Astronomy
ETH Zurich, Switzerland

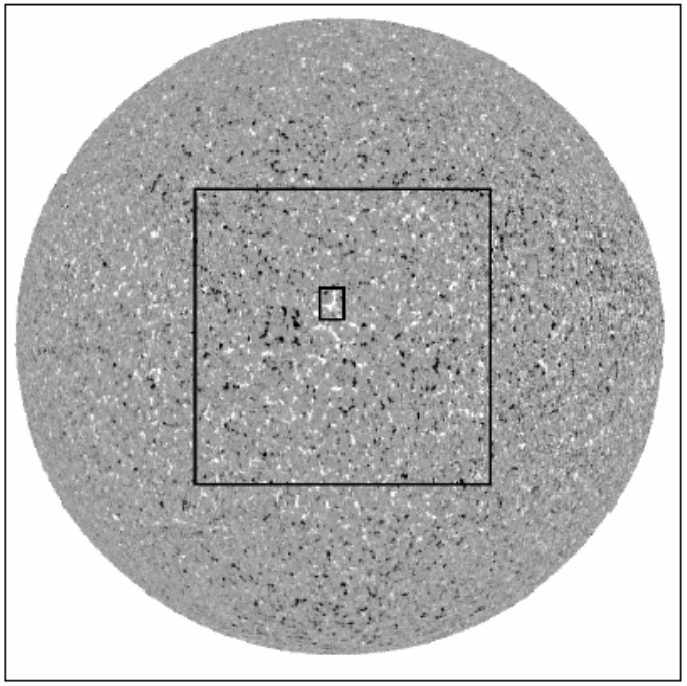

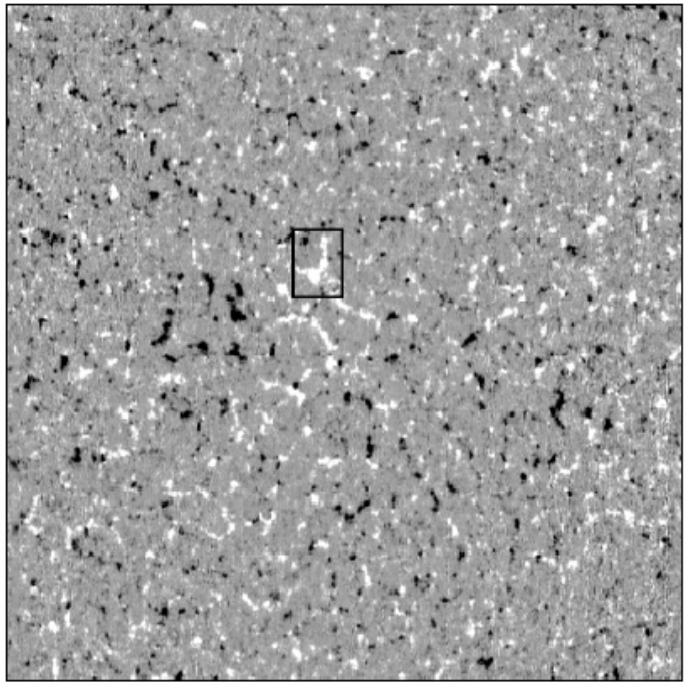

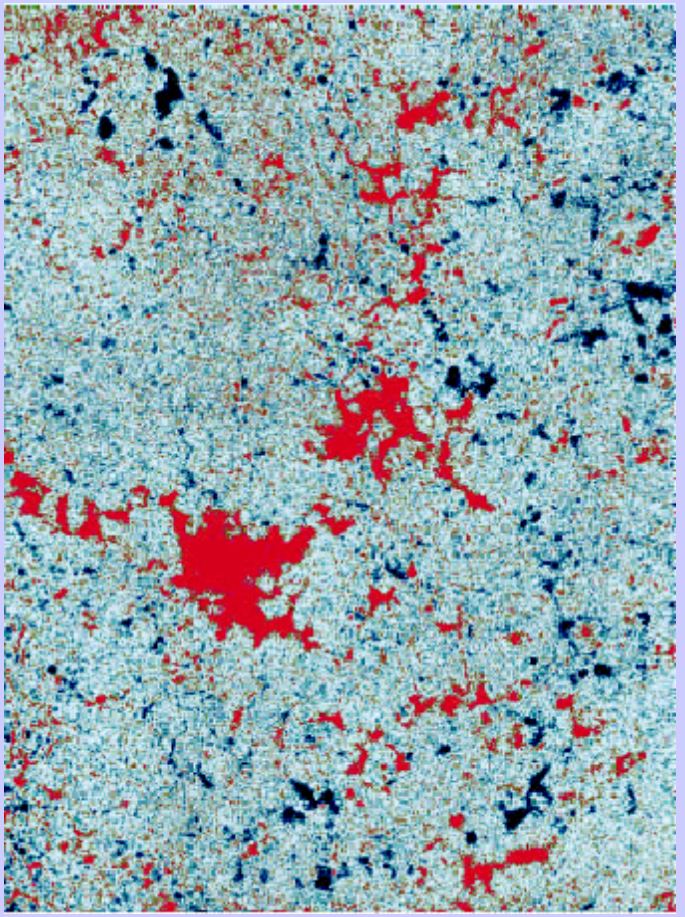

Institute of Astronomy ETH Zurich

100 years cosmic magnetic fields

George Ellery Hale discovered 1908 the Zeeman splitting in sunspots

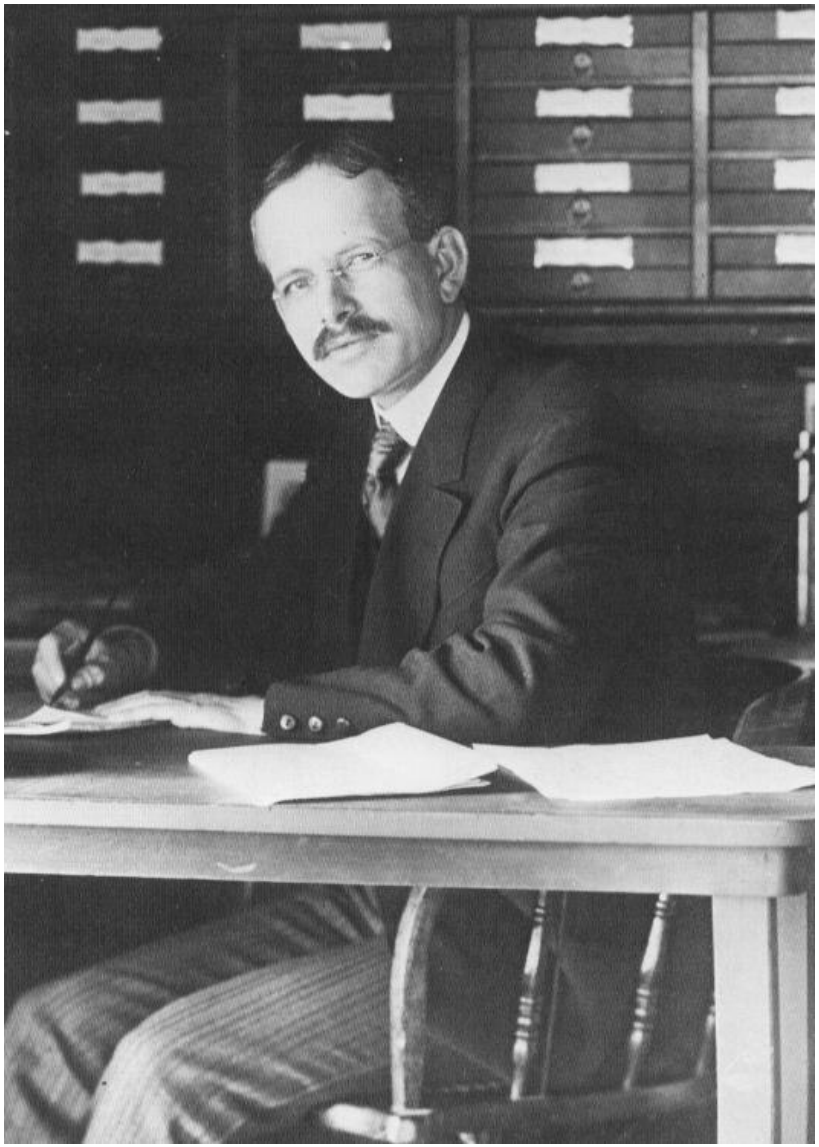

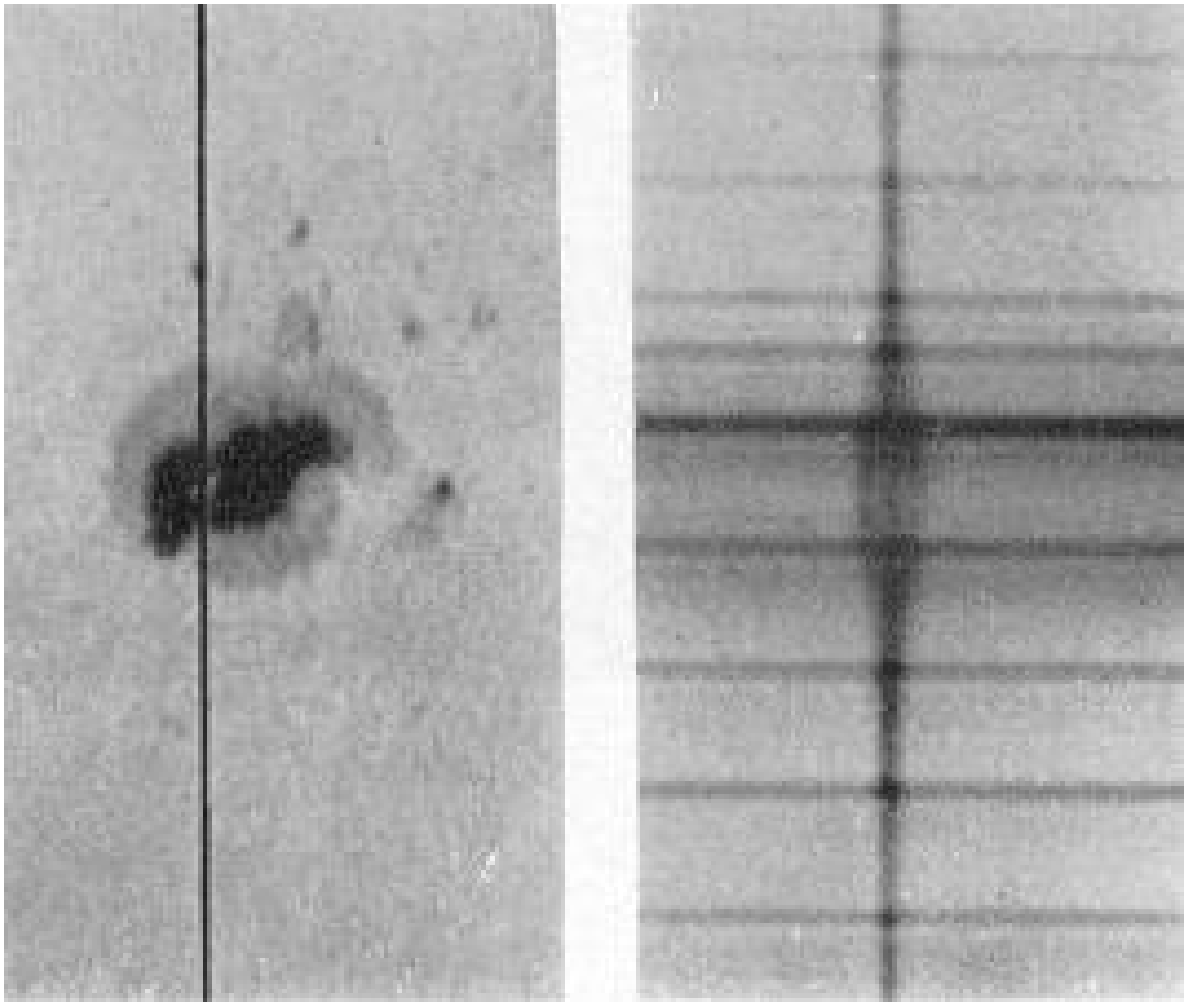

H.W. Babcock 1953, The Solar Magnetograph, ApJ 118, 387

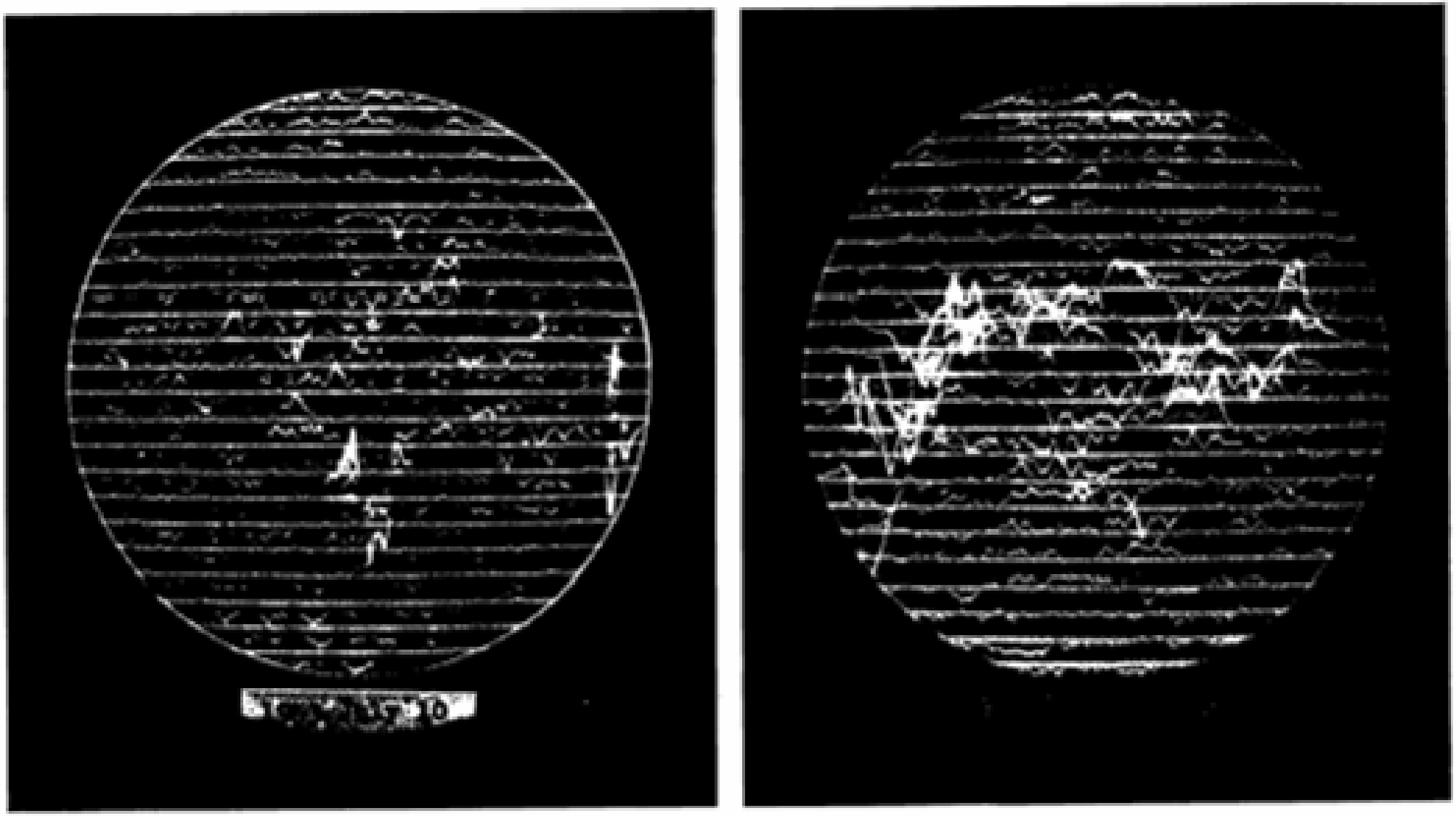

FIG. 5.—Magnetograms of the sun. The axis is vertical, with north at the top. East is at the right. For each trace there is a straight fiducial line. A deflection equal to the interval between traces indicates that $H \cos \gamma$ is about 1 gauss at the center of the disk, 2 gauss at the limb. For upward deflections $H \cos \gamma$ is toward the observer. Evidence for the sun's general magnetic field is shown by the opposite deflections on the traces nearest the north and south poles. The only visible sunspot group on July 19 was at 54° W., 8° S. The length of the slit (0.04 of the sun's diameter) is approximately equal to the interval between traces.

Institute of Astronomy ETH Zurich

Magnetograms of the active and quiet Sun

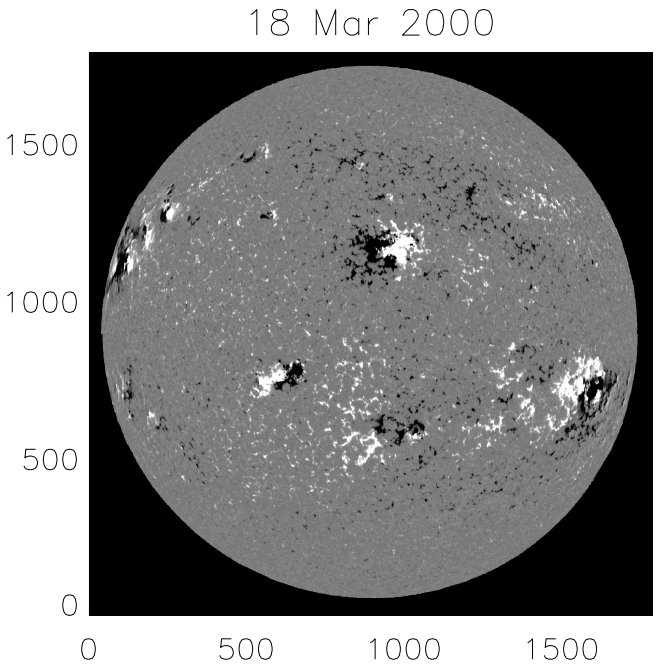

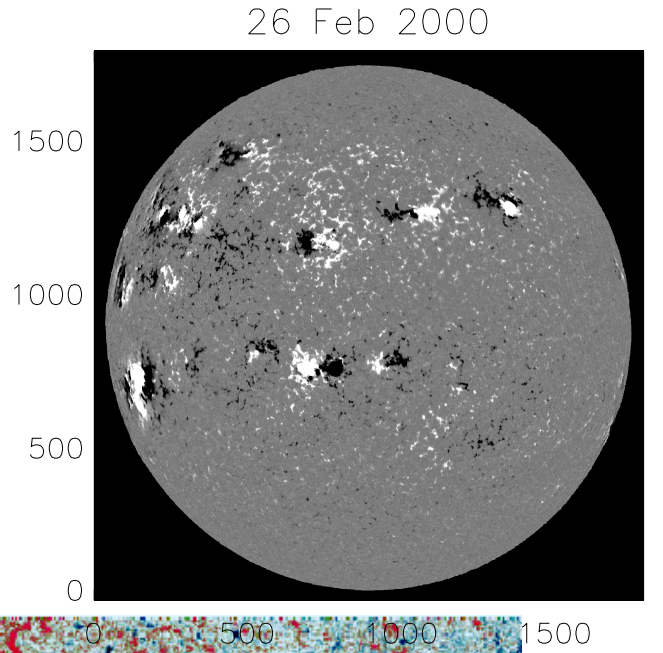

Question: What would the field look like with infinite resolution

To answer this question the line-ratio technique was introduced in 1971

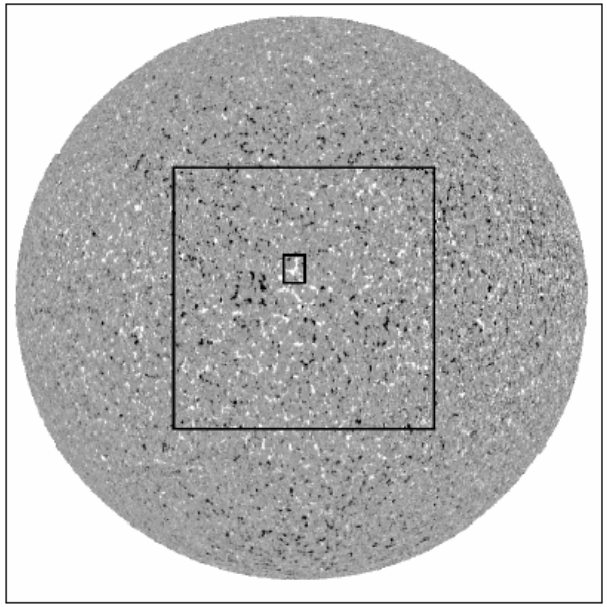

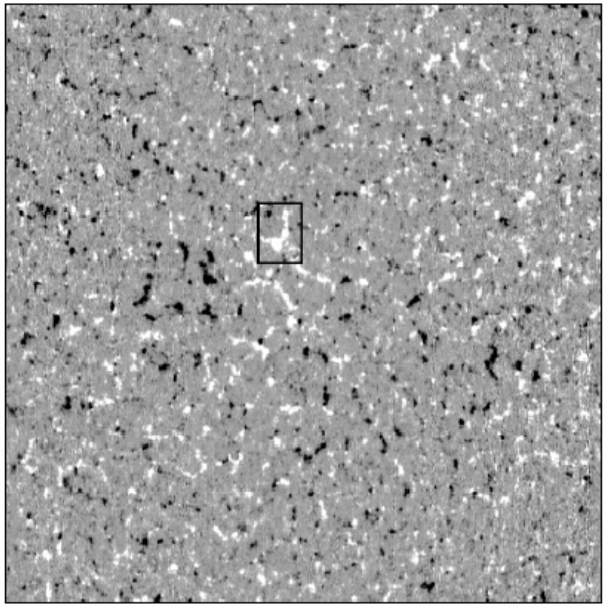

9 February 1996

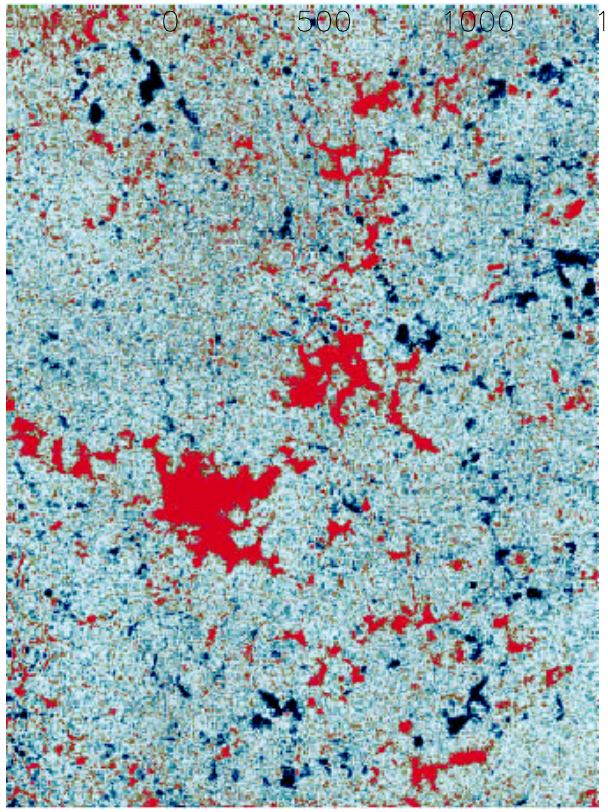

5250 / 5247 line ratio technique

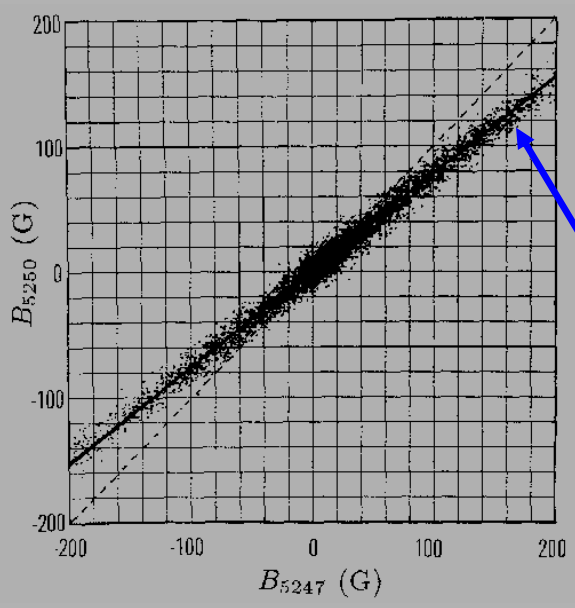

Slope gives intrinsic field strength

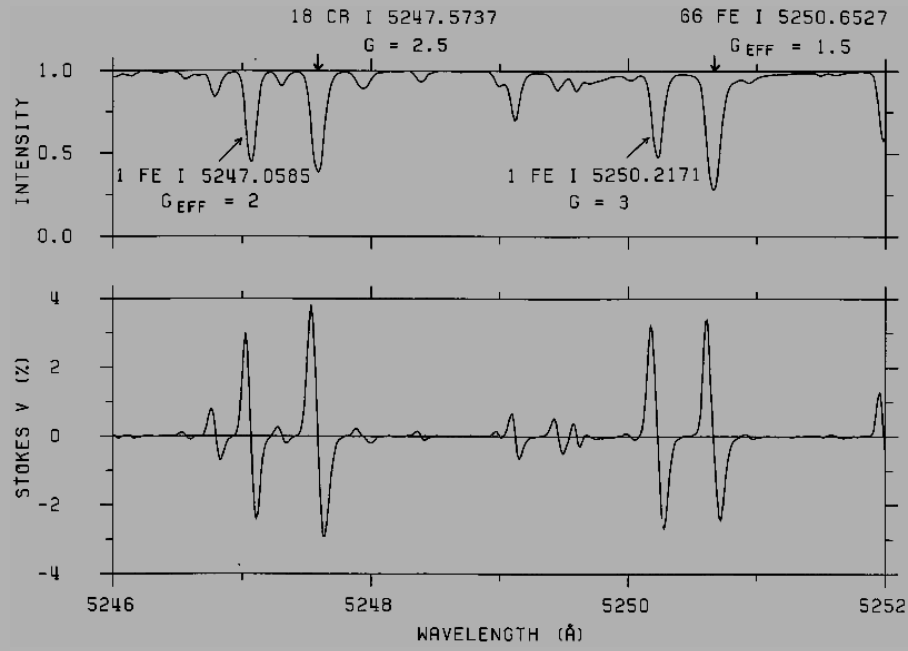

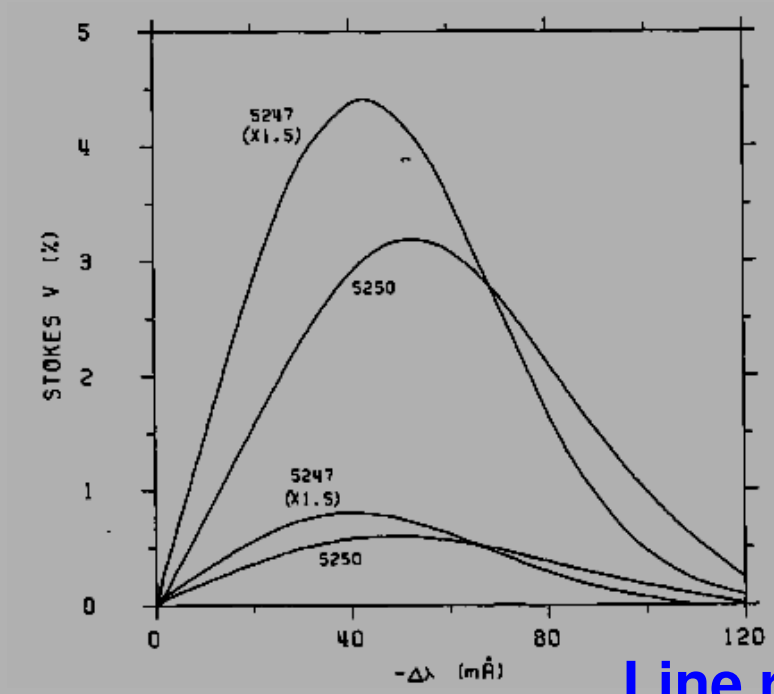

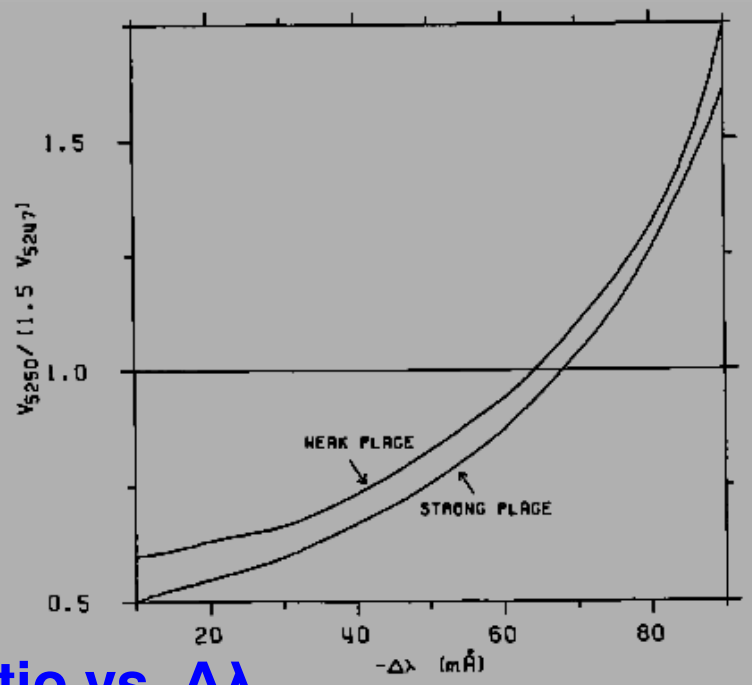

Line ratio vs. Δλ

(verifies physical validity of the model)

For the interpretation of the line-ratio data a 2-component model was introduced

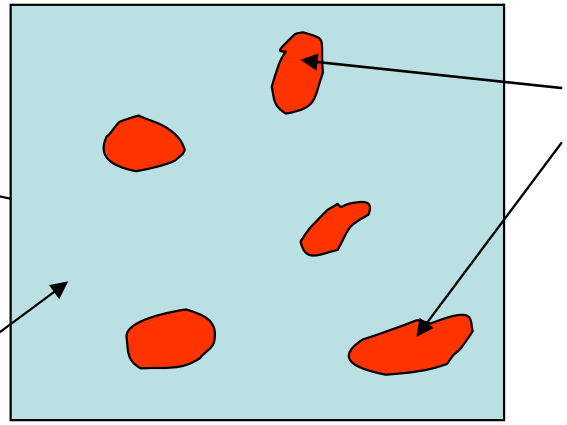

$$< B > = aB$$

Since with the two-component model B is found to be 1 - 2 kG, while a is typically about 1%, the concept of intermittent magnetic flux tubes was introduced

The flux tubes became the theoretical counterpart of the 2-component model

Institute of Astronomy ETH Zurich

Example of flux tube modeling based on spatially unresolved observations

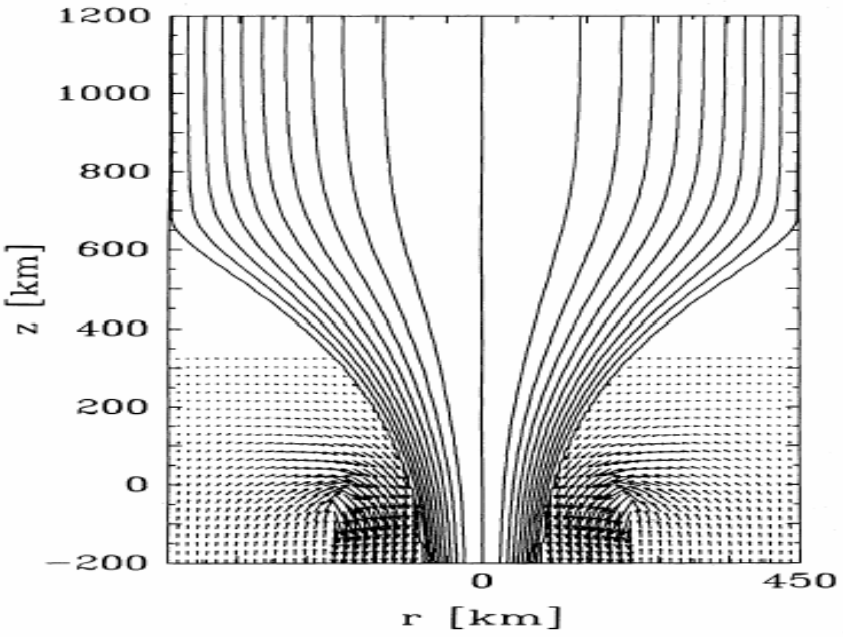

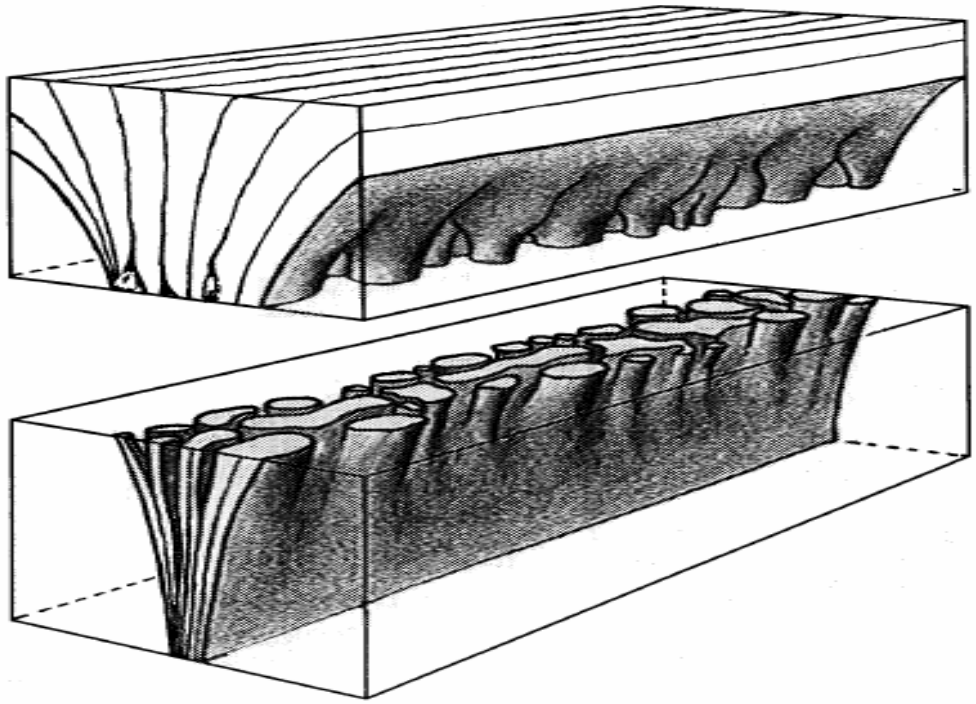

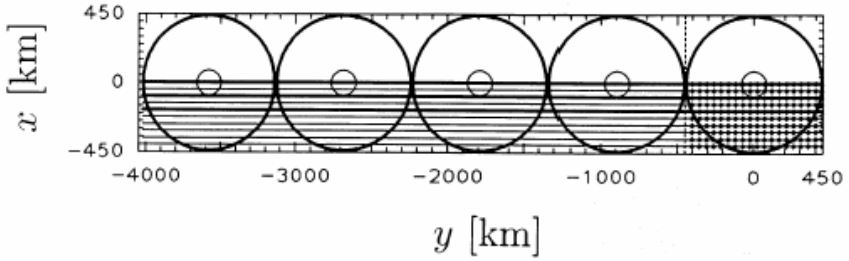

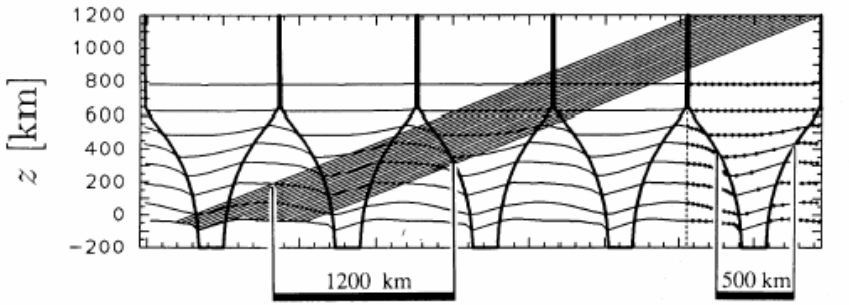

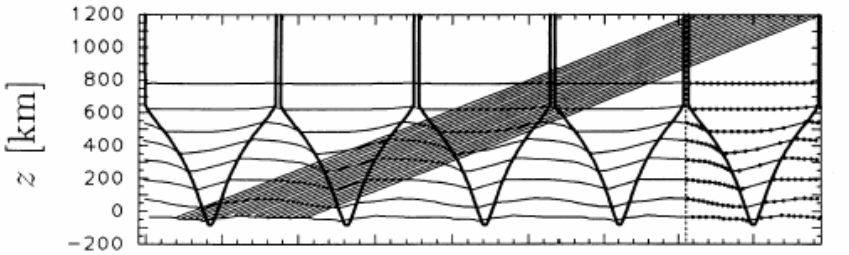

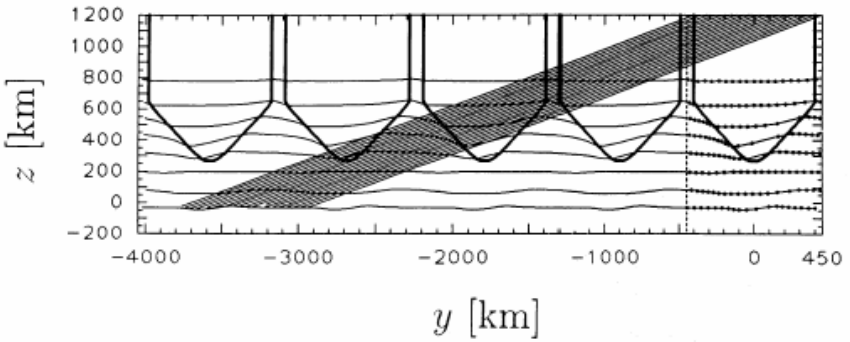

M. Bünte, A&A 276, 236 (1993), M. Bünte et al., A&A 268, 736 (1993)

Institute of Astronomy ETH Zurich

Evidence for the validity of the 2-component model came from

- **linearity and small spread of the points in the scatter plot,**
- **profile shape of line ratio (from FTS data) as theoretically expected,**
- **uniqueness of line-ratio values, later supported by infrared data.**

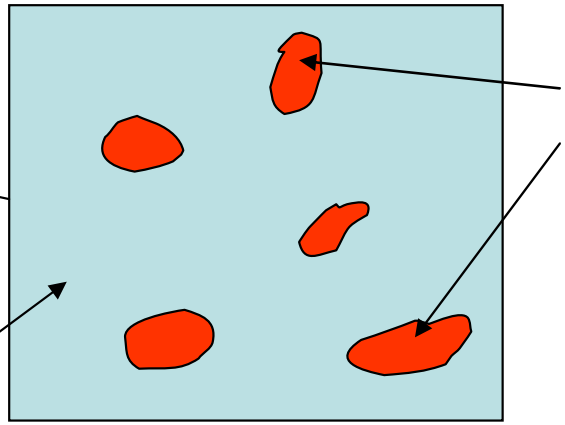

Implication: Non-magnetic component occupying 99% of the volume !!

However, it was from the beginning clear that the concept of a "non-magnetic" component is unphysical in the highly conducting solar atmosphere. It was only introduced for mathematical convenience to bring out the flux tube component.

The next quest therefore was to determine the magnetic properties of this "hidden" component.

This problem found its solution with the Hanle effect.

Institute of Astronomy ETH Zurich

Wilhelm Hanle visits ETH Zurich in 1983 on the occasion of the 60th anniversary of his effect, discovered in Göttingen in 1923

Topic of discussion:
Quantum interference between the Ca II H and K lines, recorded at Kitt Peak in 1978

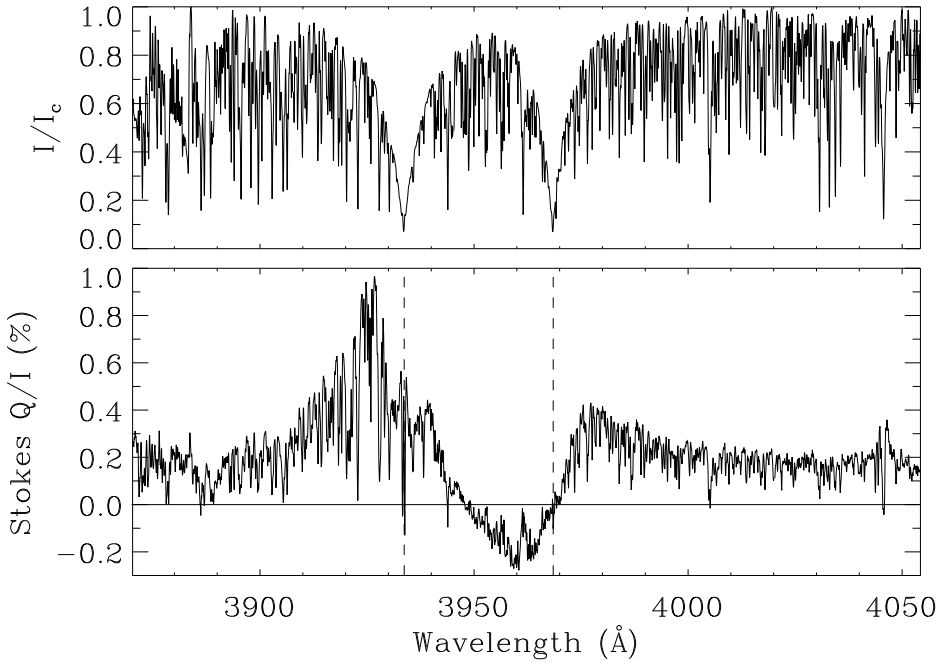

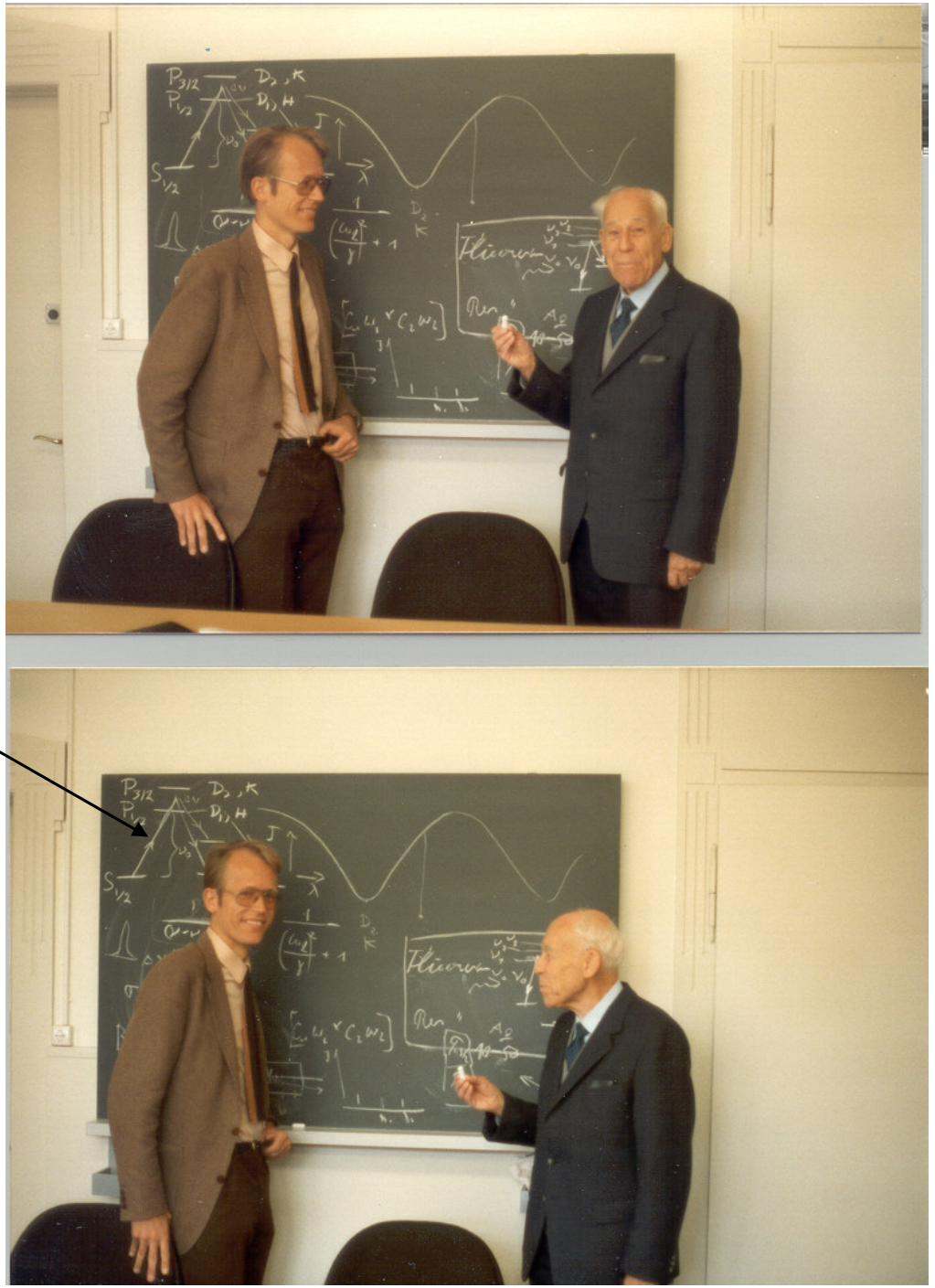

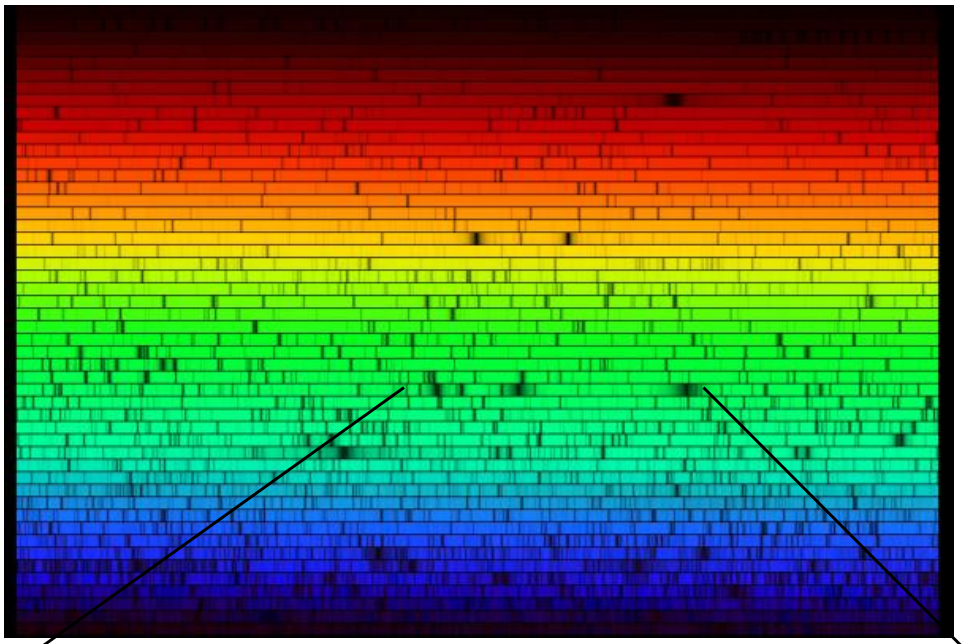

ZIMPOL (Zurich Imaging Polarimeter)
allows vector polarimetry with a polarimetric precision of 10^{-5}.

This opens the door to the "Second Solar Spectrum"

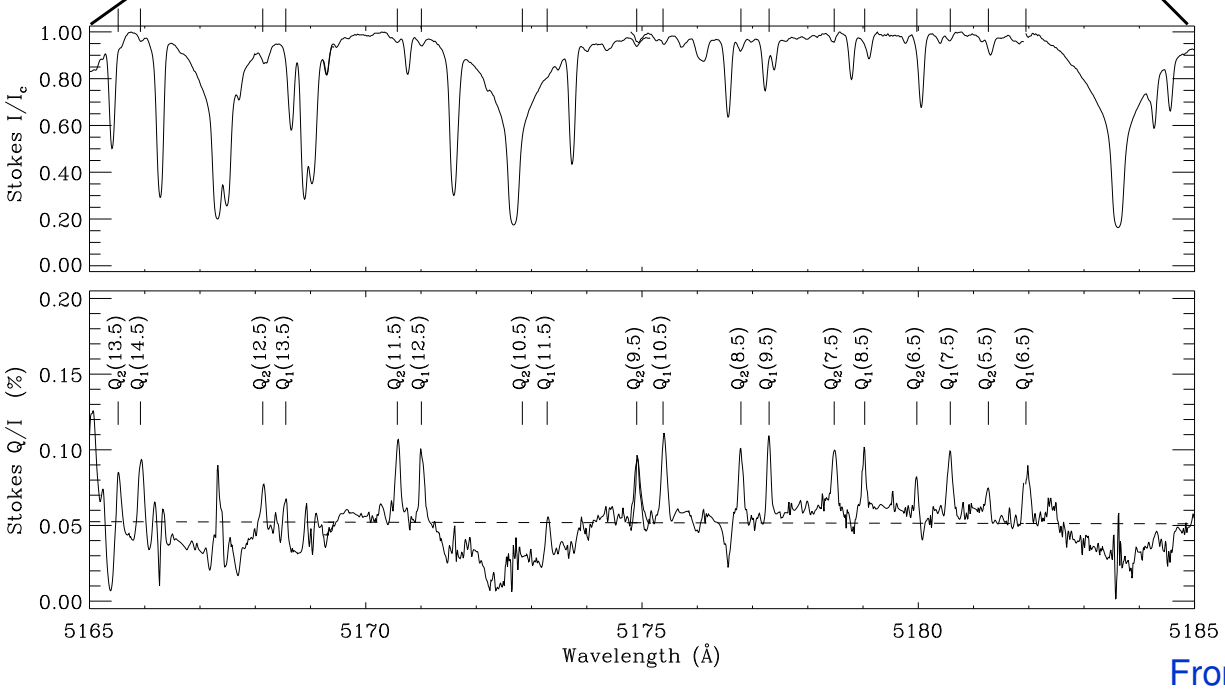

First solar spectrum

Second solar spectrum

From Gandorfer's Atlas

Institute of Astronomy ETH Zurich

Linear polarization pattern across the solar disk due to non-magnetic coherent scattering.

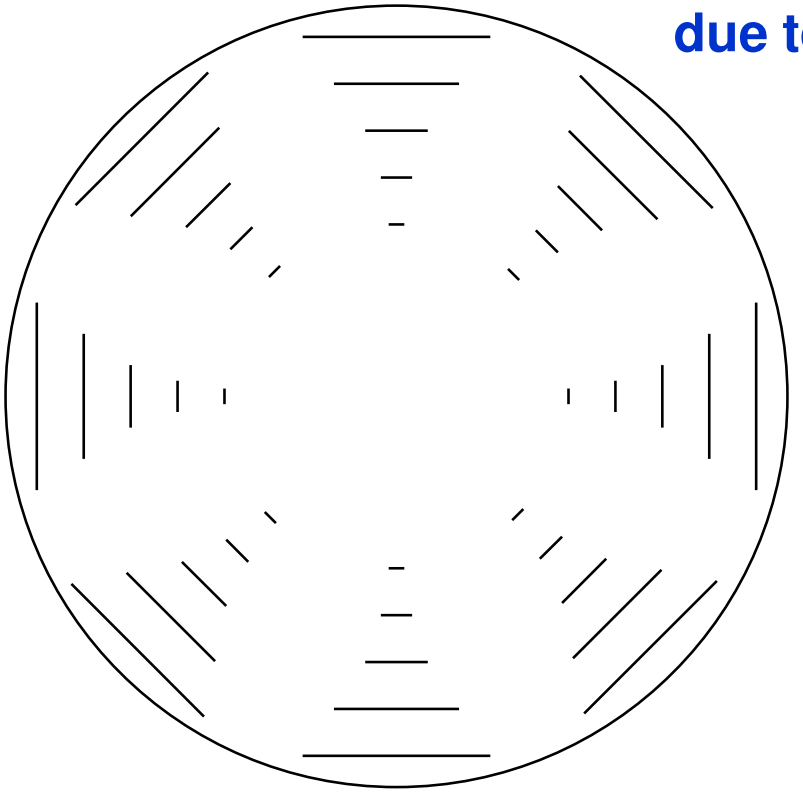

The incident radiation field is anistropic due to the limb darkening.

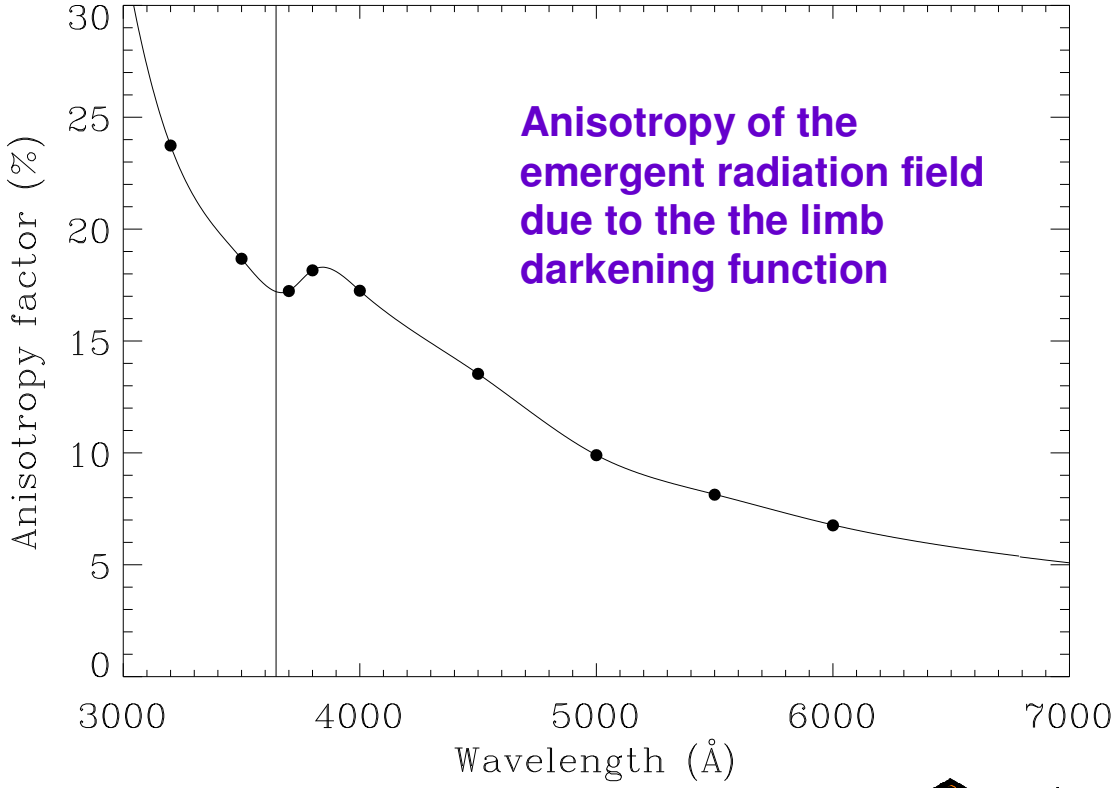

Hanle effect

Influence of magnetic fields on the scattering polarization

Precession of the oscillator around the magnetic field vector

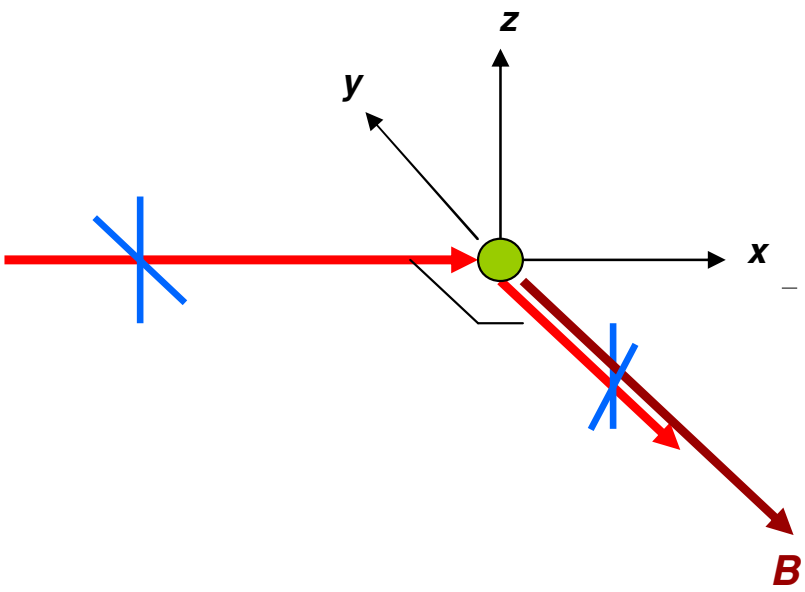

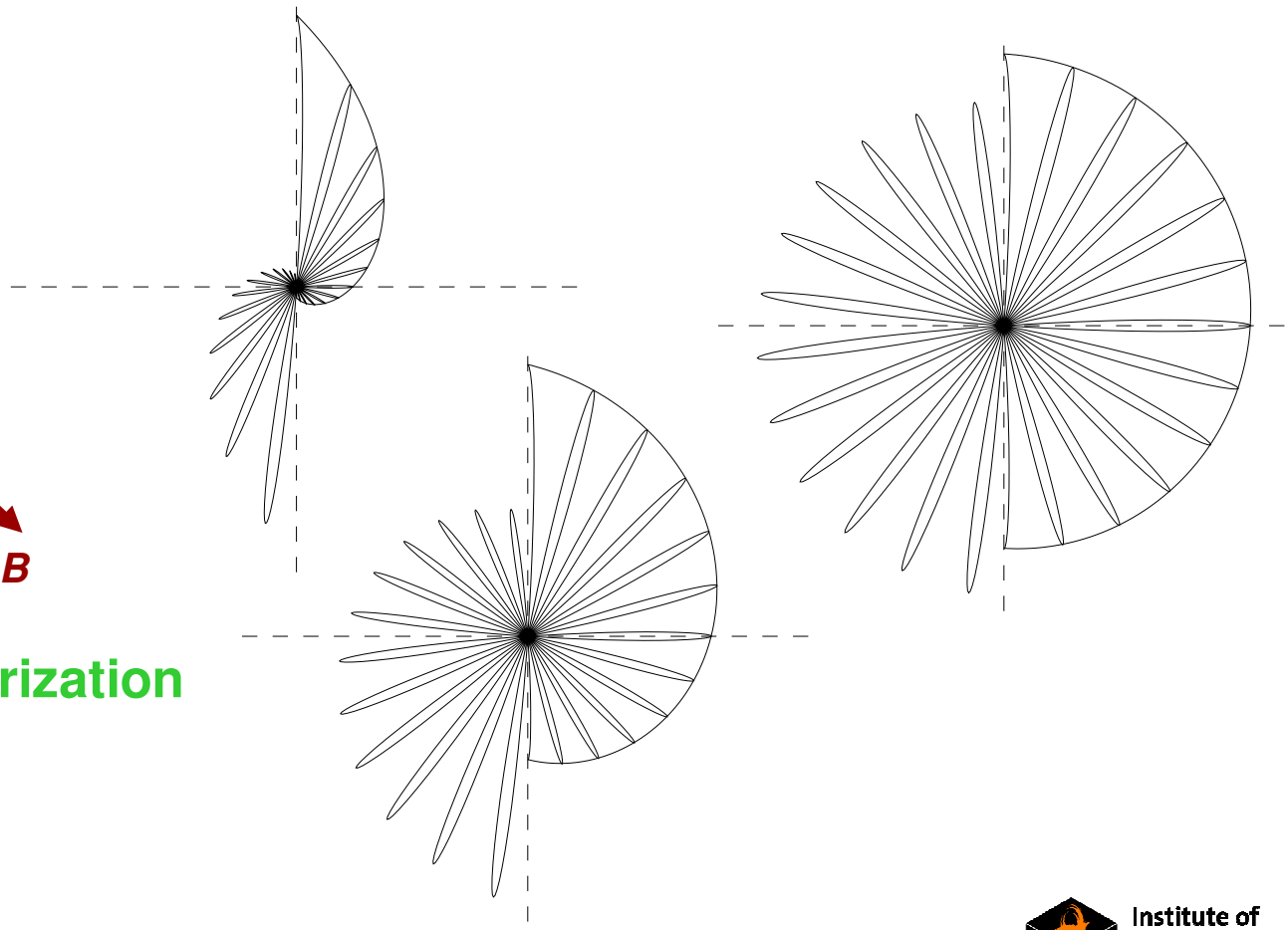

Two main effects:

- **Rotation of the plane of polarization**
- **Depolarization**

Hanle effect

Precessing classical oscillator

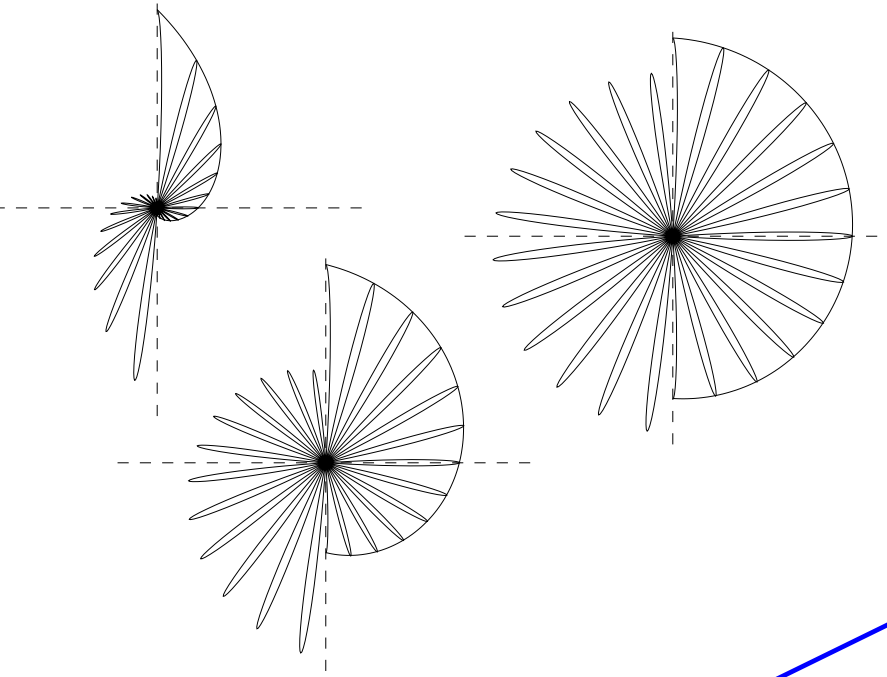

Hanle depolarization and rotation of the plane of polarization in the line core

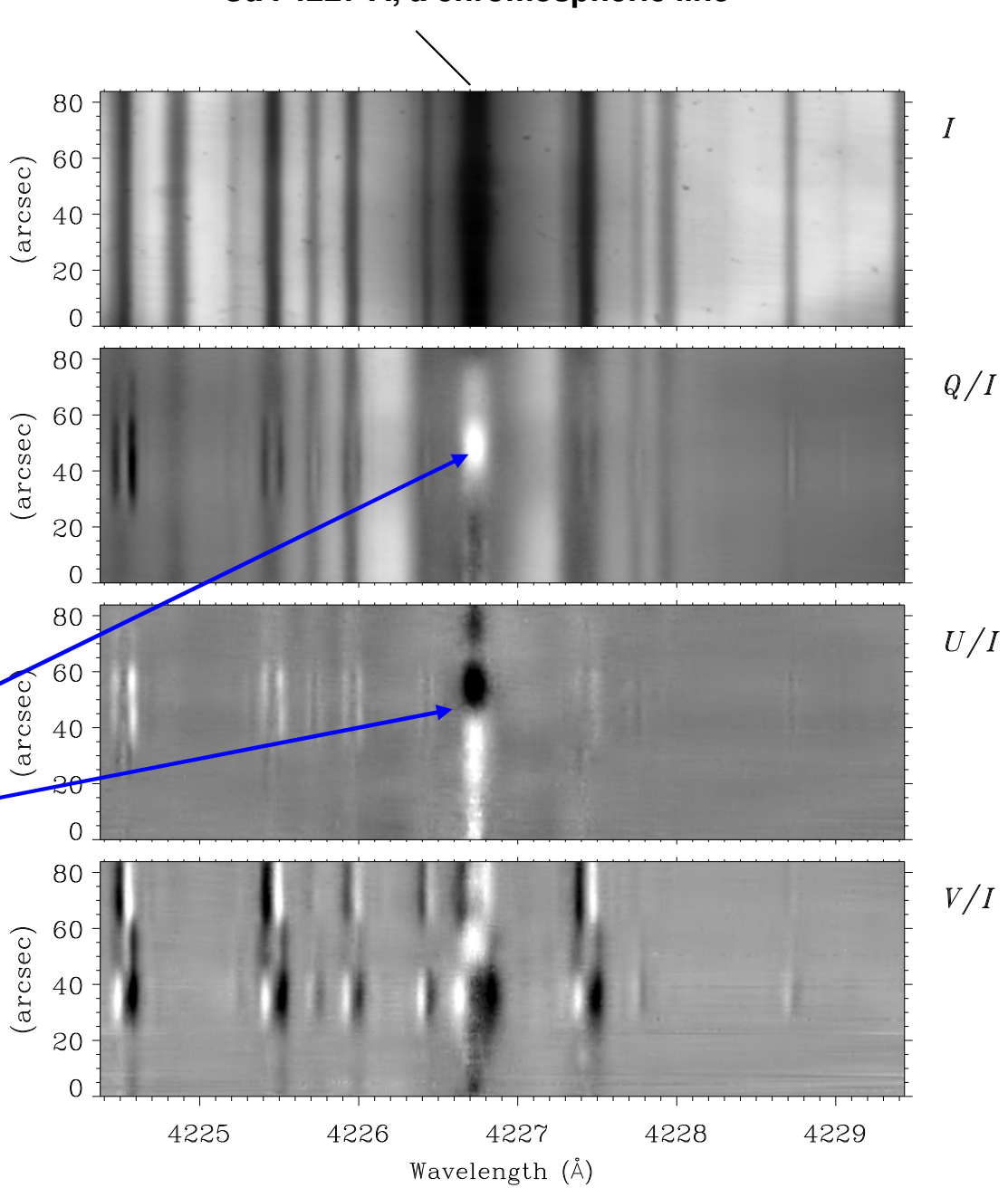

Difference in Hanle signatures between photospheric and chromospheric lines

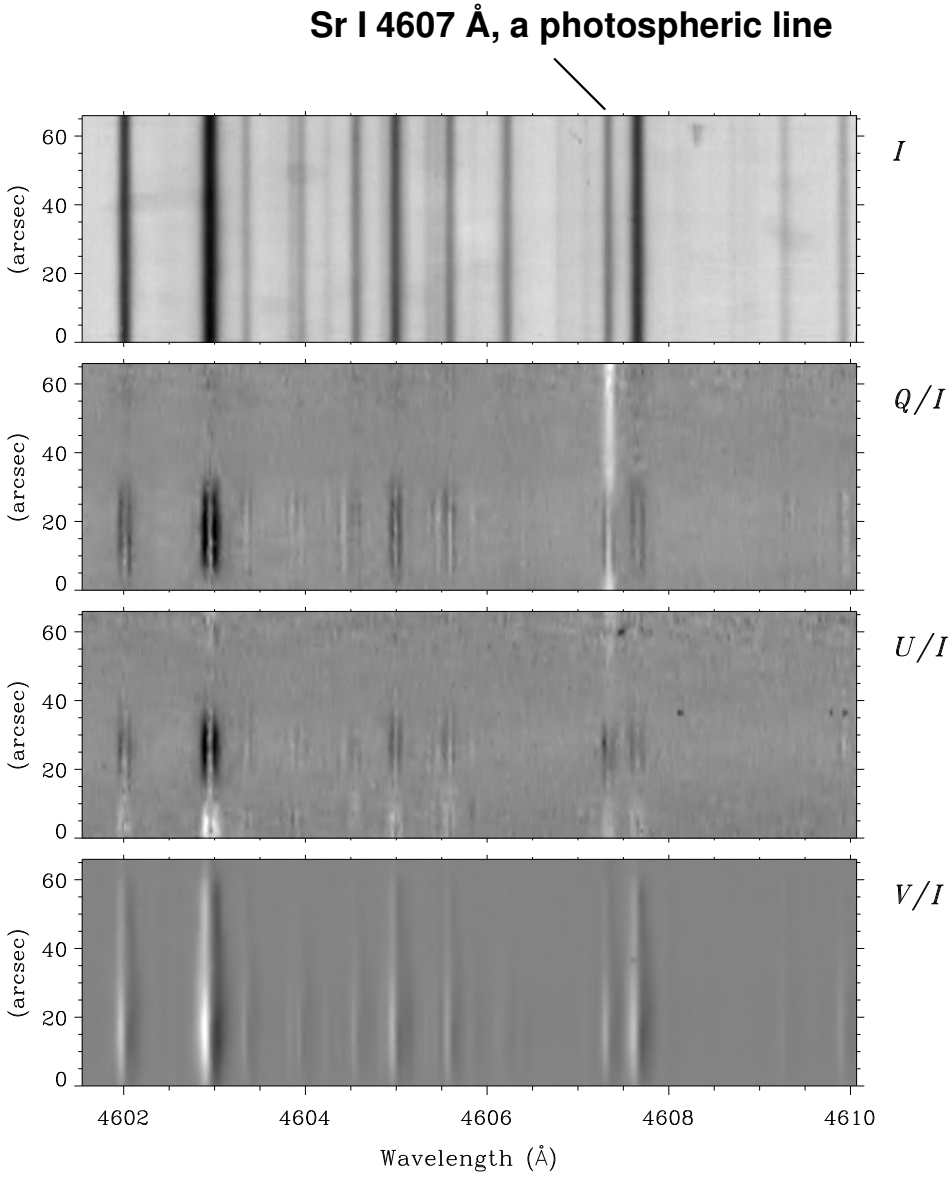

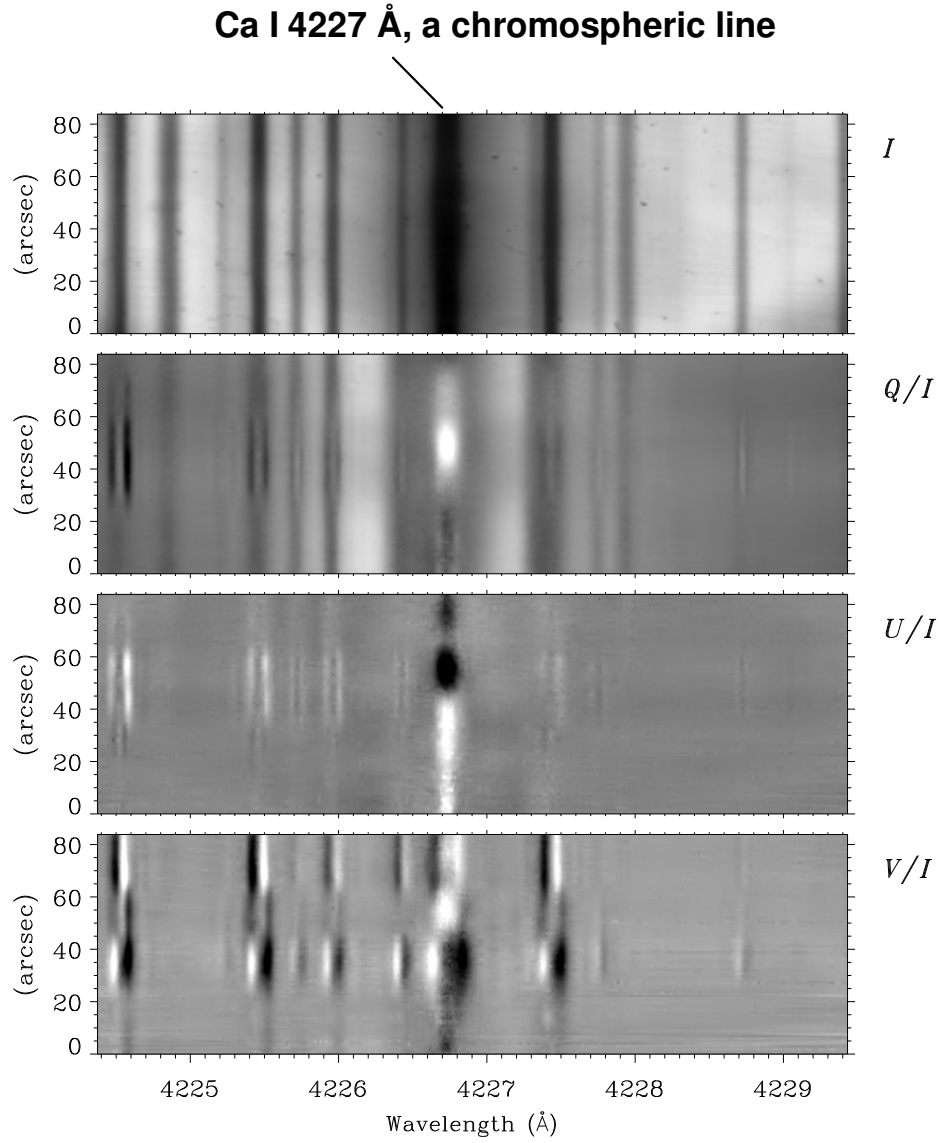

Scattering polarization in CN lines in magnetic environments: 3771 – 3775 Å

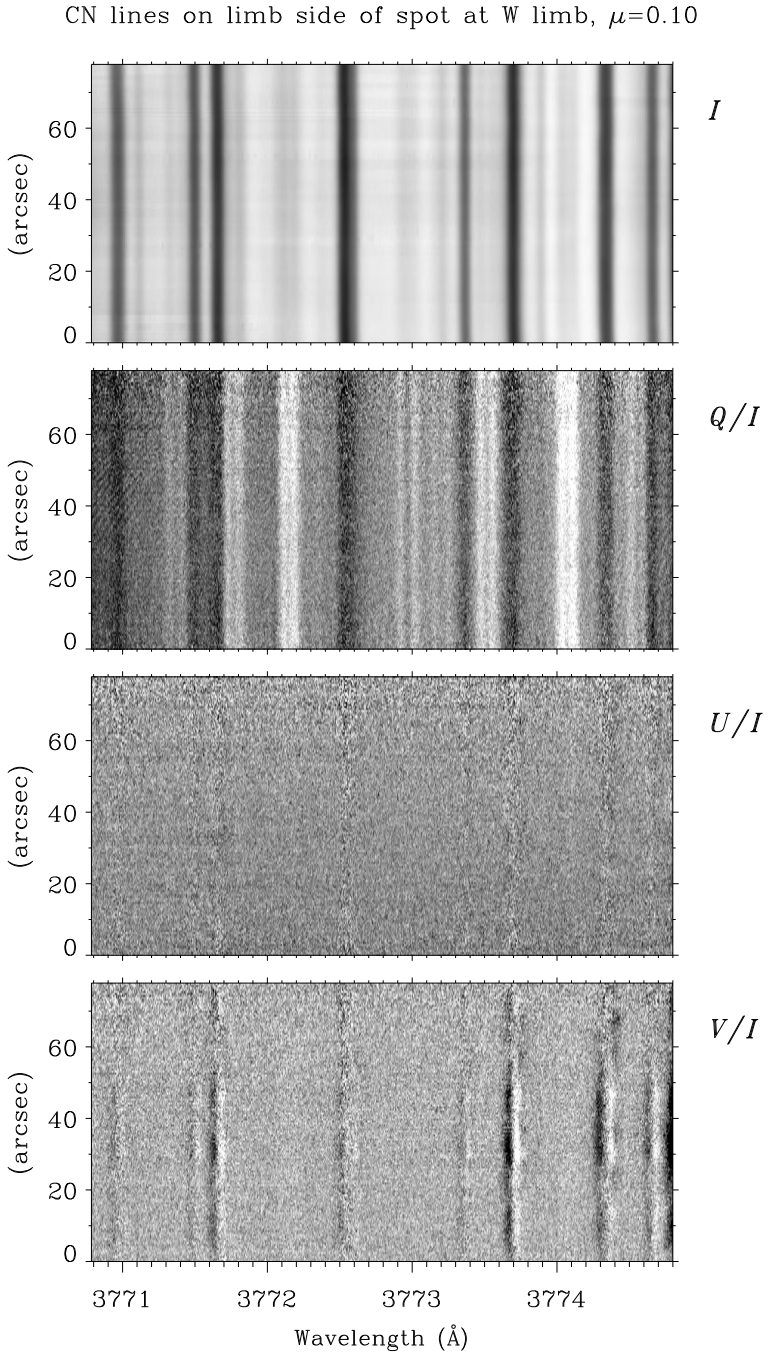

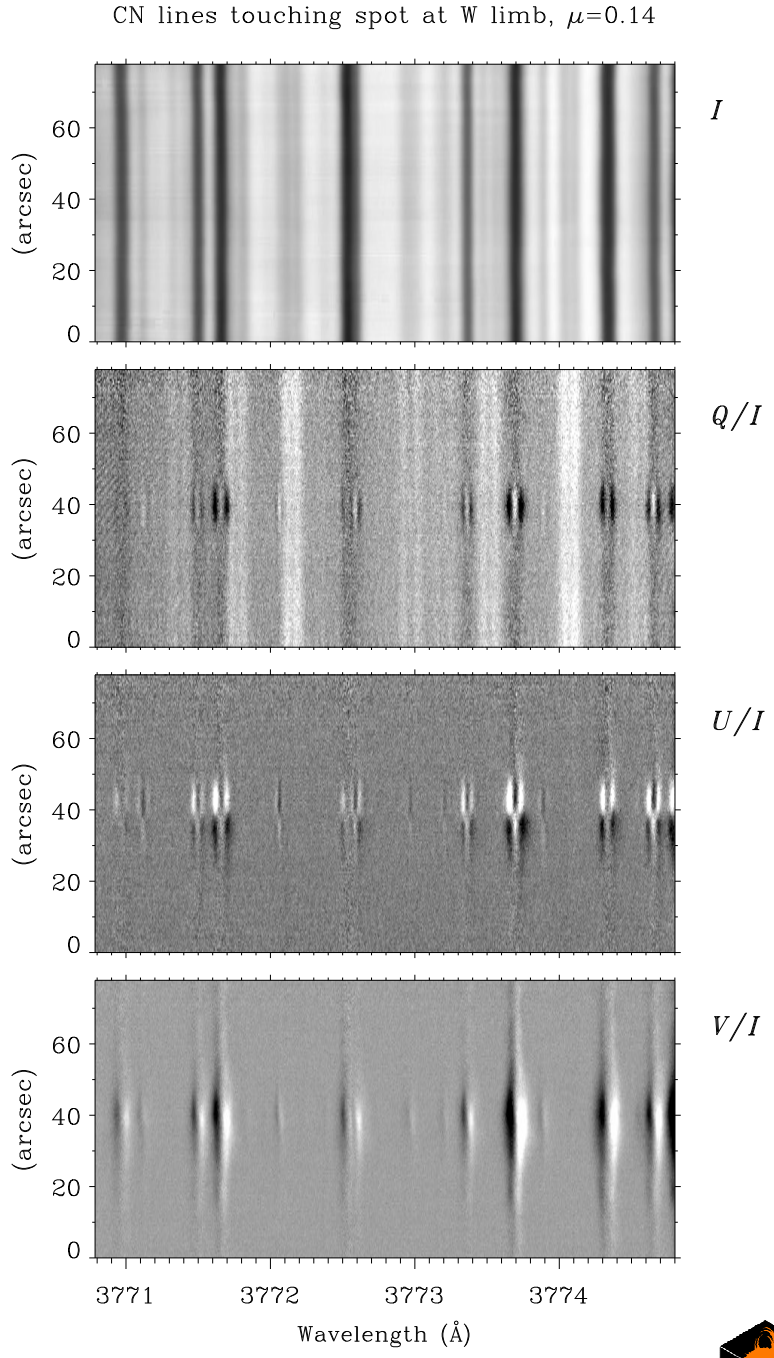

J.O. Stenflo

Institute of Astronomy
ETH Zurich

Extension of the 2-component model through use of the Hanle effect

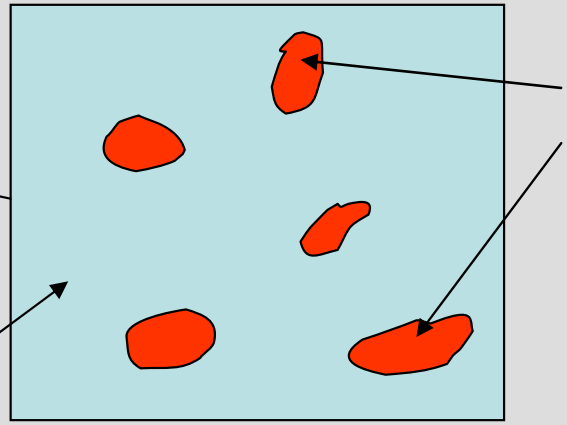

Spatial resolution element

Magnetic component,
filling factor a,
field strength B

Not a "non-magnetic" atmosphere
but a mixed-polarity, tangled
or turbulent field

Institute of Astronomy ETH Zurich

Resulting "standard model"

- **Flux tubes expanding with height, forming canopies above the photosphere. Contribute to the Zeeman effect.**
- **Weaker tangled or turbulent field in between. No information from the Zeeman effect, but accessible with the Hanle effect.**

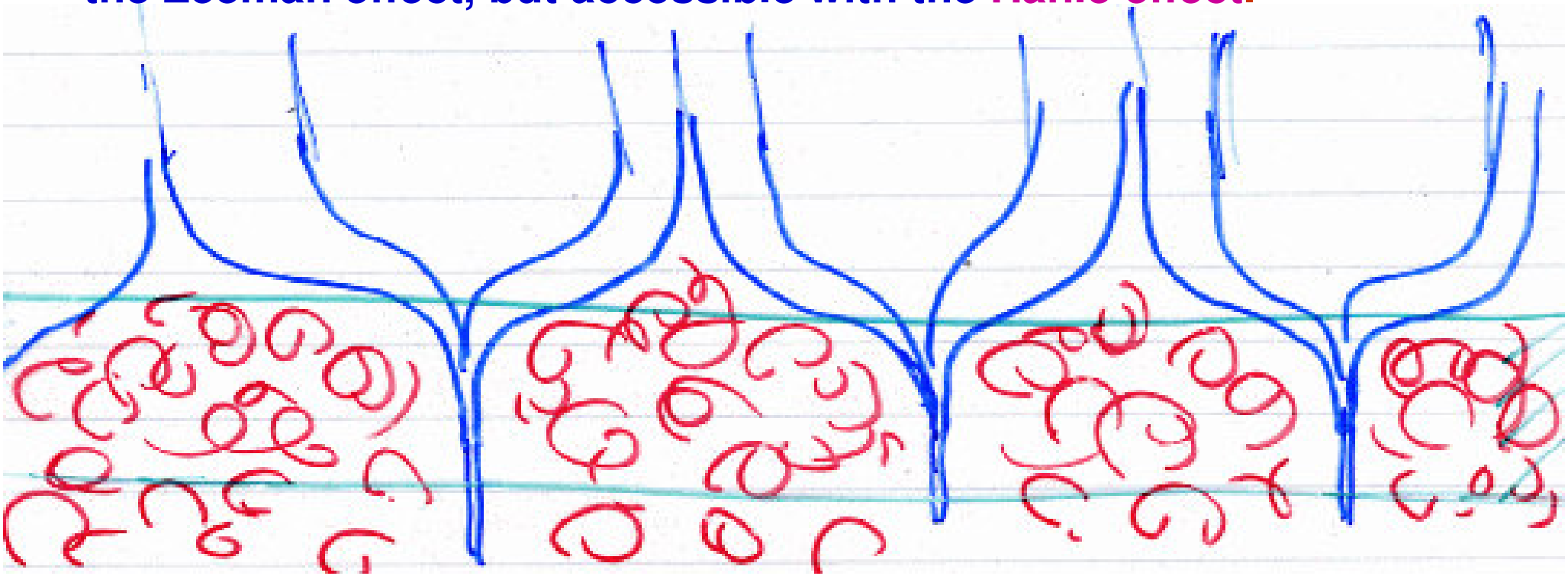

This dualistic scenario is however an artefact of applying two diagnostic tools, which are highly complementary: the Zeeman and Hanle effects.
The real world is not dualistic.

Institute of Astronomy ETH Zurich

New paradigm: fractal magnetic fields,

described by probability distribution functions (PDFs)

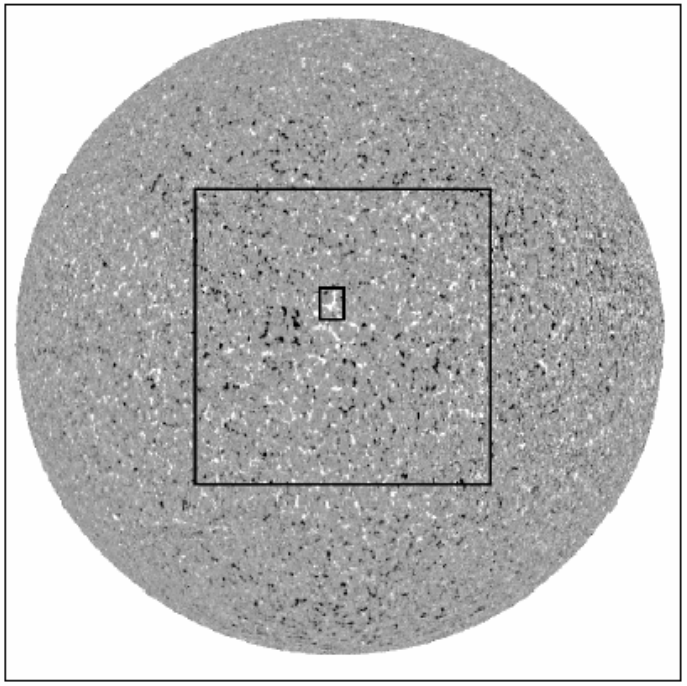

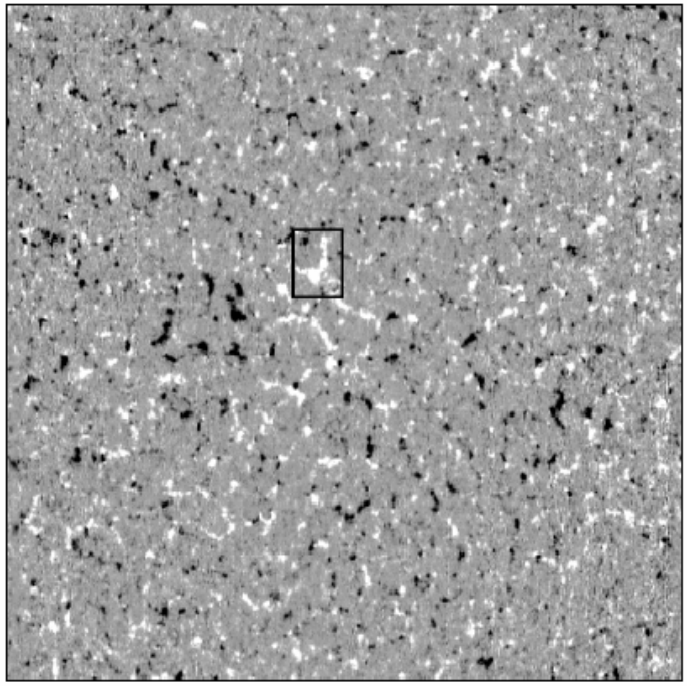

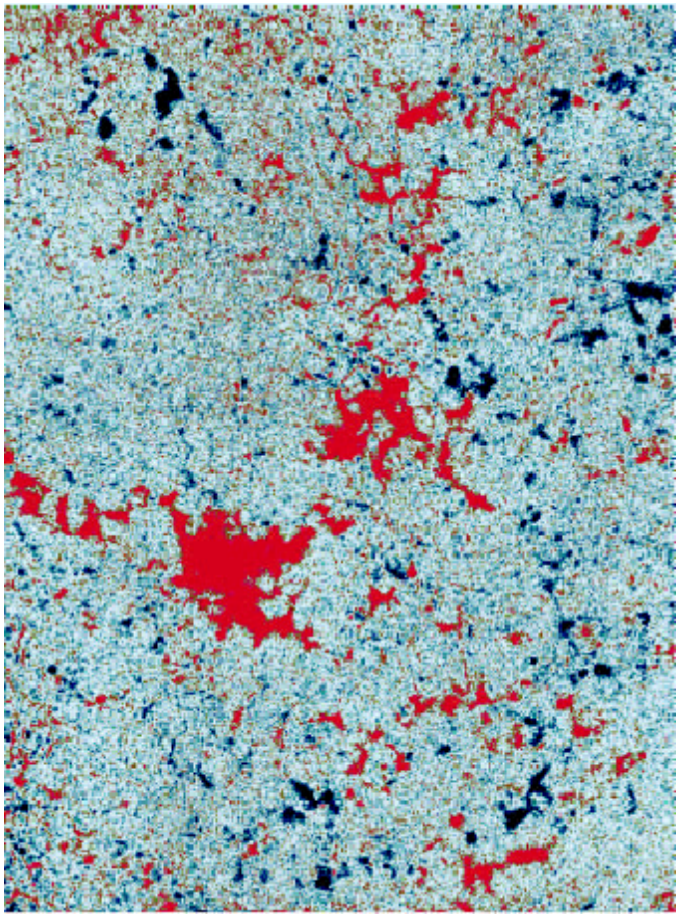

La Palma magnetogram
9 February 1996

MDI magnetogram
20 March 2002

The area of the left magnetogram is only 0.35 % of the area covered by the right one (scale in arcsec)

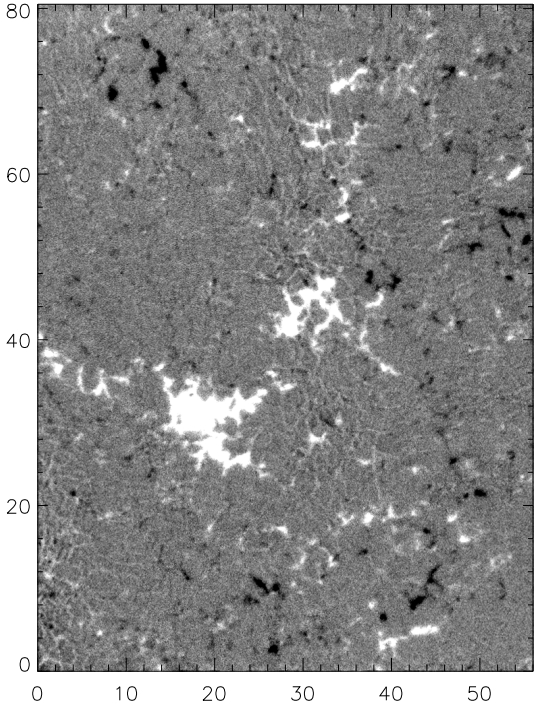

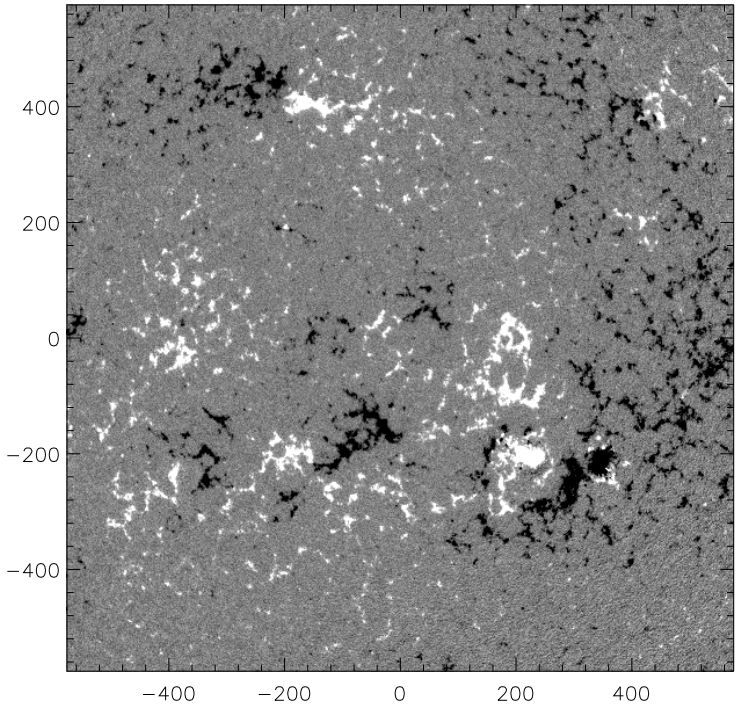

Fractal patterns

Empirical PDFs:
La Palma (thick), MDI (thin),
Voigt profile (dashed)

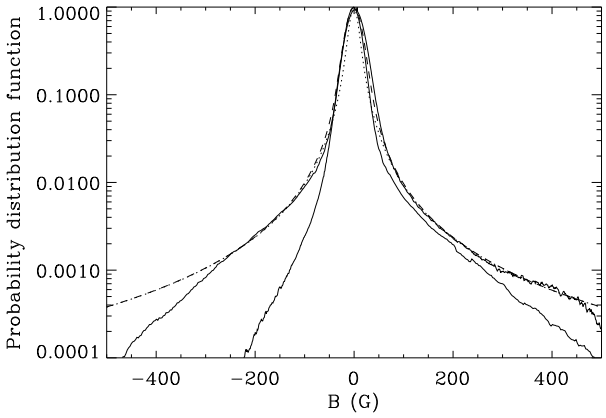

Comparison between theory (Stein & Nordlund 2002;
solid line for B_z, dashed line for $|B|$)
and the empirical Voigt function (dotted)

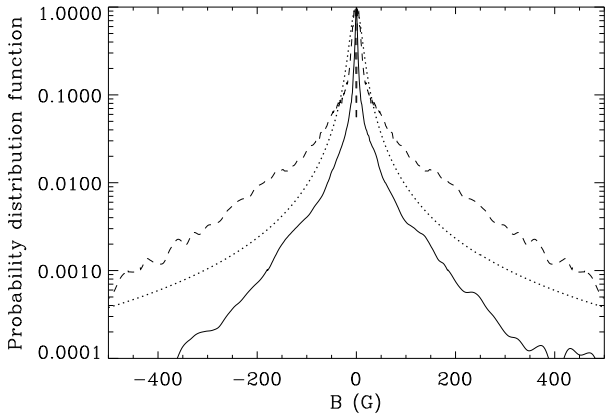

Probability distribution functions PDF

From Stenflo & Holzreuter 2002

Estimate of the lower end of the scale spectrum

Magnetic Reynolds number

$$R_m = \mu_0 \sigma \ell_c v_c$$

Spitzer conductivity

$\sigma = 10^{-3} T^{3/2}$ (SI units)

Kolmogorov turbulence (inertial range)

$v_c = k \ell_c^{1/3}$ (where k is a constant)

With $R_m = 1$ at the diffusion limit, and $k = 25$ (corresponding to 2.5 km/s for $\ell_c = 1000$ km), we get

$$\ell_{diff} = 1 / (\mu_0 \sigma k)^{3/4} \text{ , or}$$

$$\ell_{diff} = 5 \times 10^5 / T^{9/8}$$

For T = 10,000 K we get

$$\ell_{diff} = 15 \text{ m}$$

Institute of Astronomy ETH Zurich

Fractal magnetic fields on the quiet Sun

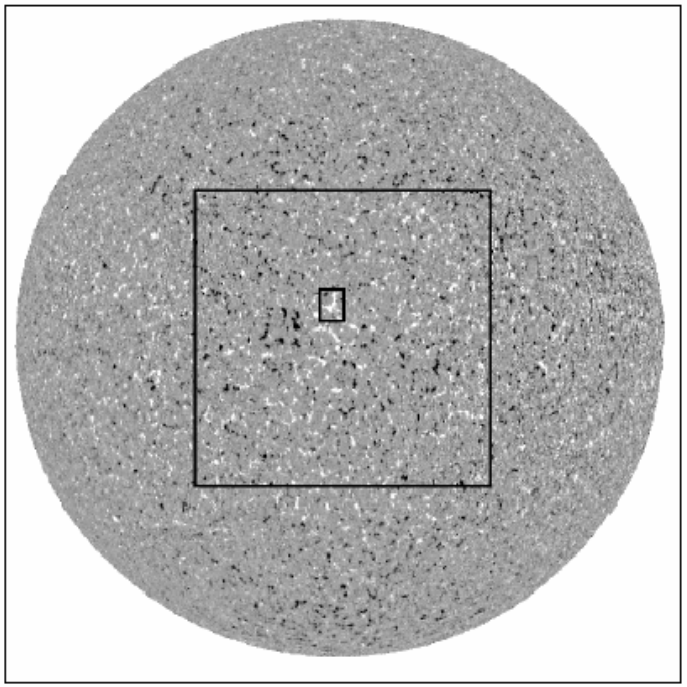

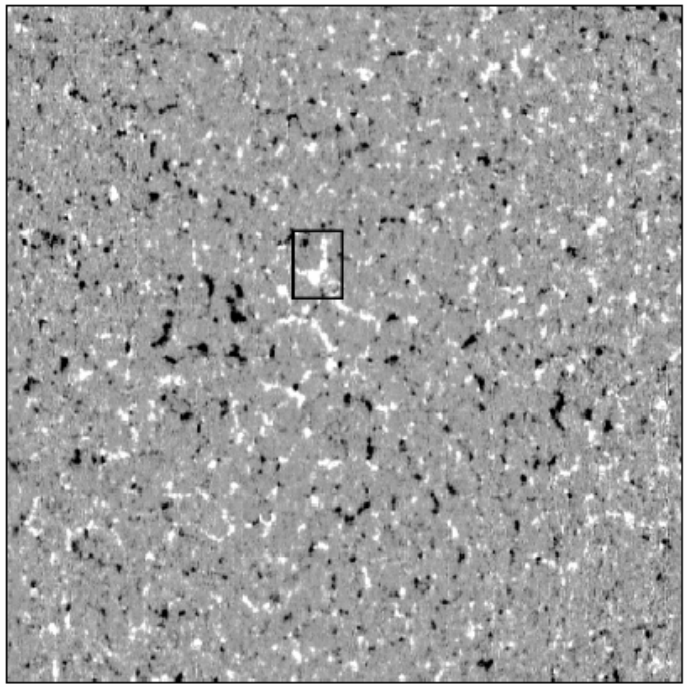

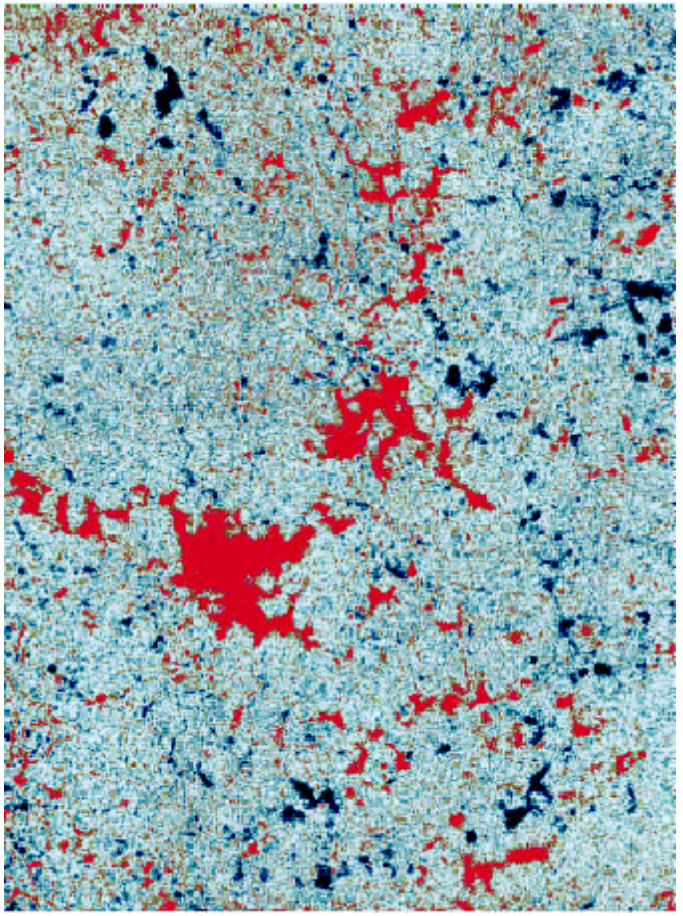

The apparent voids are no voids at all, but are teeming with turbulent magnetic fields (*Trujillo Bueno, Shchukina, Asensio Ramos ; Stenflo Nature 2004*).

This conclusion is based on the application of the Hanle effect in Sr I 4607 Å. Assuming a certain shape of the PDF, Trujillo Bueno et al. find hidden and ubiquitous, tangled magnetic flux with an average strength of about 130 G

Institute of Astronomy ETH Zurich

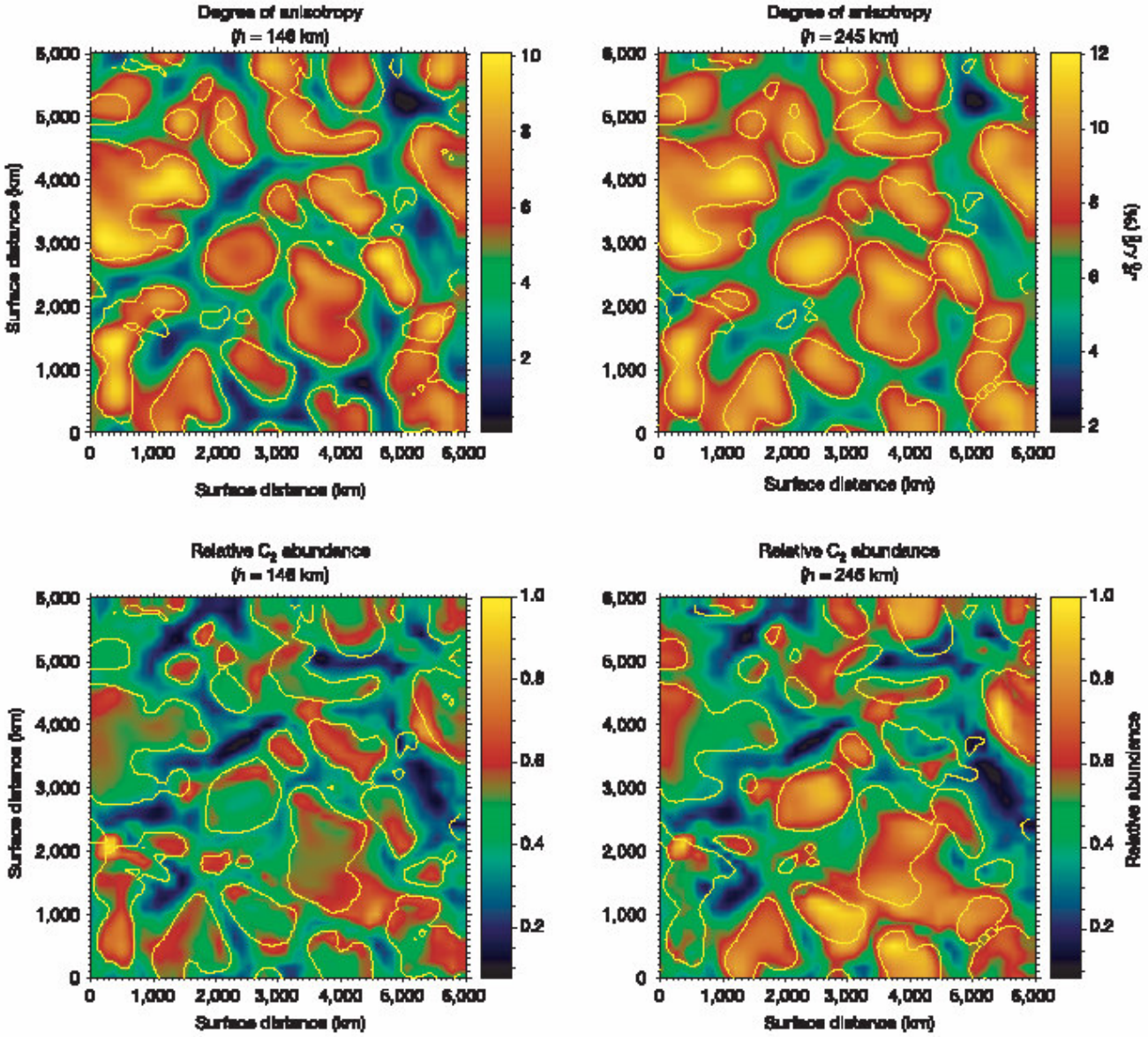

The anisotropy of the radiation field (top panels) and the C_2 abundance (bottom panels) are closely correlated with the upflowing regions in the solar granulation

Trujillo Bueno, Shchukina, and Asensio Ramos (2004) conclude from comparing Sr I and C_2 Hanle depolarization that the turbulent field is strongly localized in the intergranular lanes.

Institute of Astronomy ETH Zurich

Diagnostic tools for dealing with magnetic probability distribution functions in Stokes vector observations are currently being developed at IIA in Bangalore

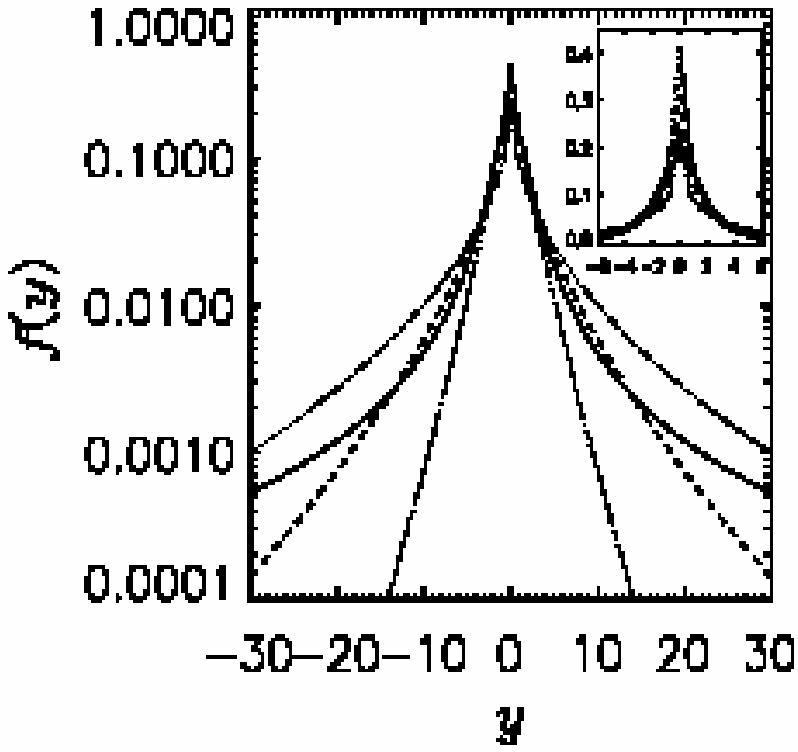

Zeeman line formation in solar magnetic fields

Studies with empirical probability distribution functions

M. Sampoorna[1,2,*], K. N. Nagendra[1,2], H. Frisch[2], and J. O. Stenflo[3]

[1] Indian Institute of Astrophysics, Koramangala, Bangalore 560 034, India
e-mail: sampoorna@iiap.res.in
[2] Laboratoire Cassiopée, CNRS, Université de Nice, Observatoire de la Côte d'Azur, BP 4229, 06304 Nice Cedex 4, France
[3] Institute of Astronomy, ETH Zürich, 8092 Zürich, Switzerland

High-precision imaging polarimetry has opened the door to a new world of observational solar physics.

- **The Second Solar Spectrum is the vast playground for the Hanle effect.**

- **It opens a new window to explorations of solar magnetism. Here I have tried to show how we need to go beyond the "standard model" to a new paradigm based on distribution functions for a fractal-like field.**

- **For the optimum choice of Zeeman-Hanle interpretational models for the "hidden" fields we need to explore the scaling laws for the distribution functions of field strength and field orientation.**

Our journey into this new world is just beginning!

Thank you !

Institute of Astronomy ETH Zurich

Examples from the “second solar spectrum”

Ca II K and H

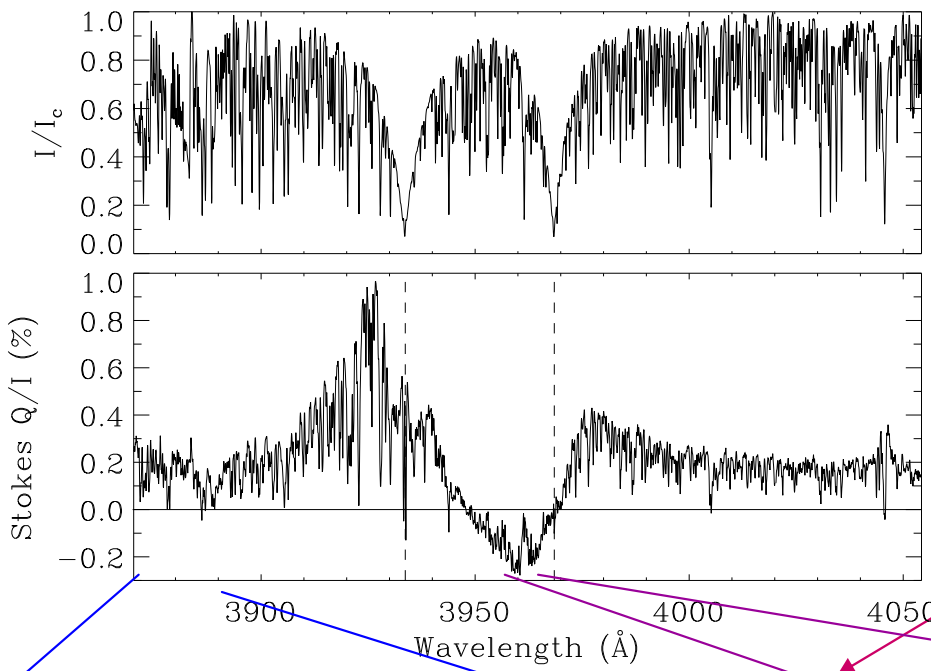

Quantum interference of the Ca II K & H scattering transitions (analogous to the double-slit experiment)

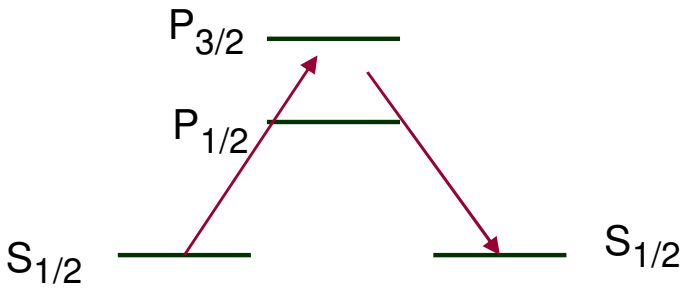

Expanded sections of the second solar spectrum

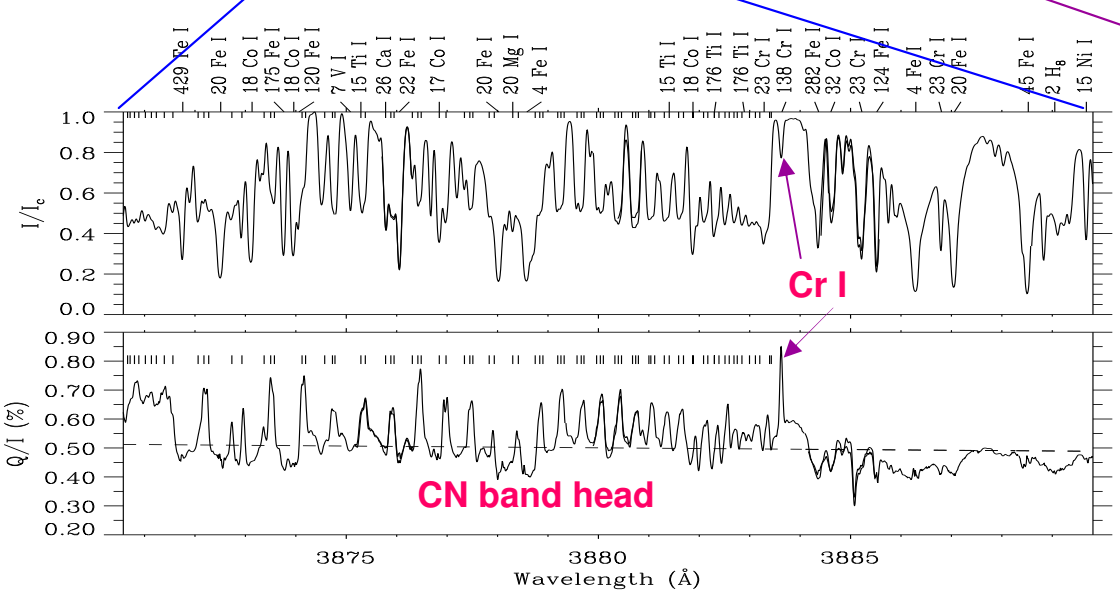

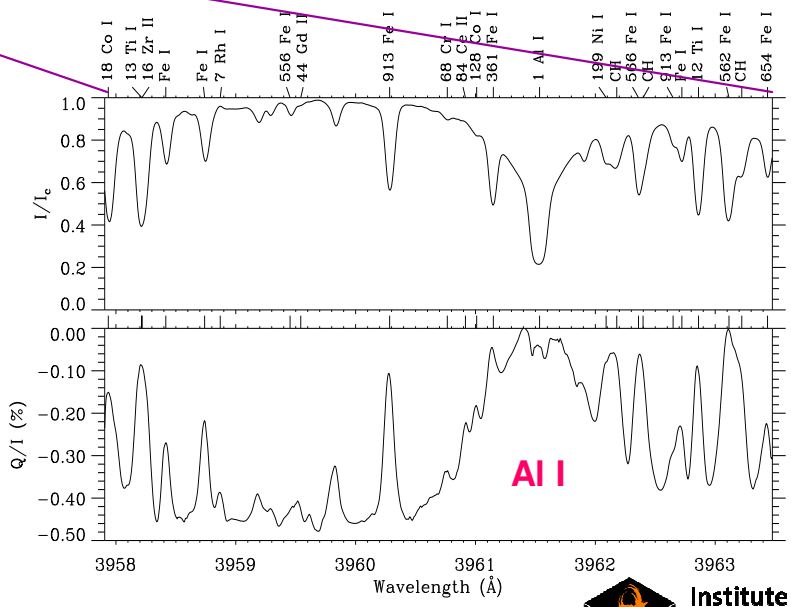

Institute of Astronomy ETH Zurich

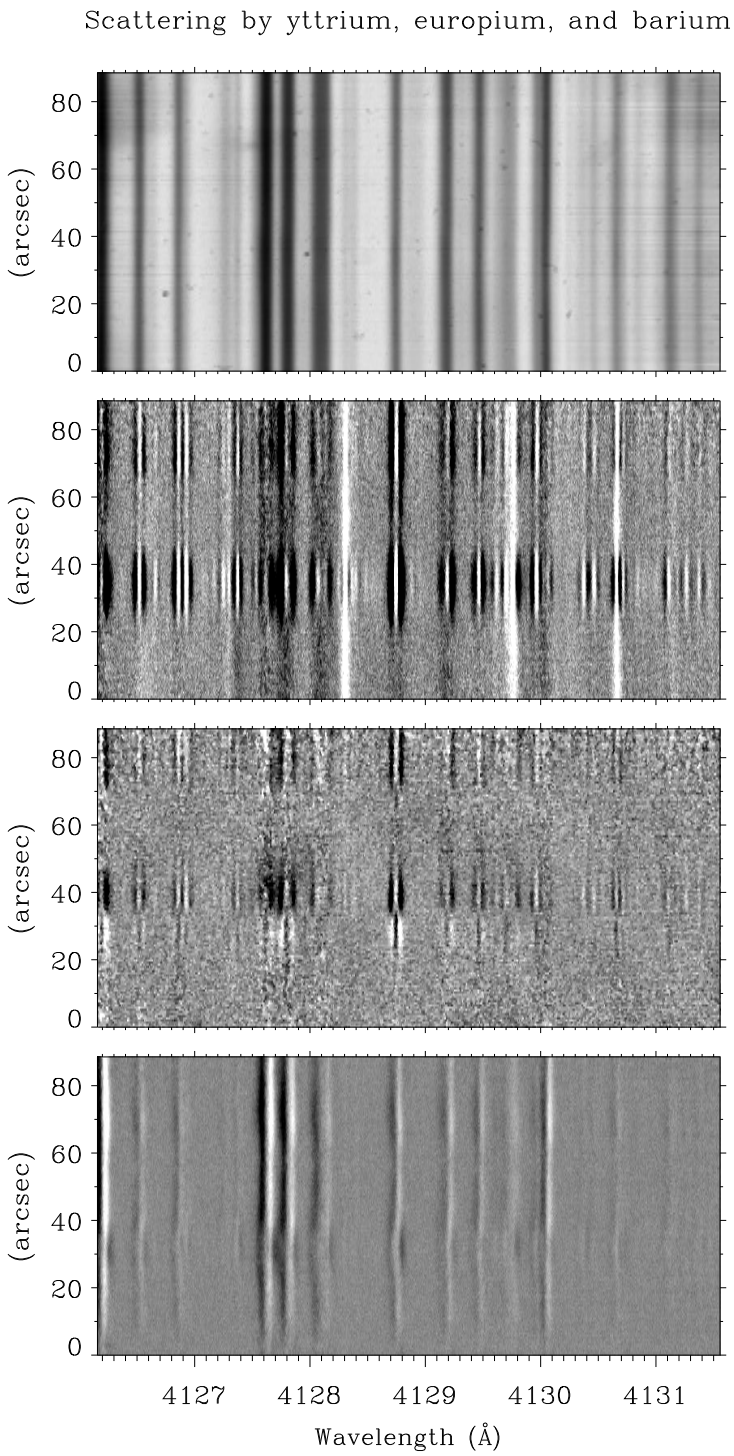

The Y I, Eu II, and Ba II lines that show pronounced scattering polarization appear to be immune to the Zeeman effect

Hyperfine structure and isotope effects

Hyperfine splitting in barium

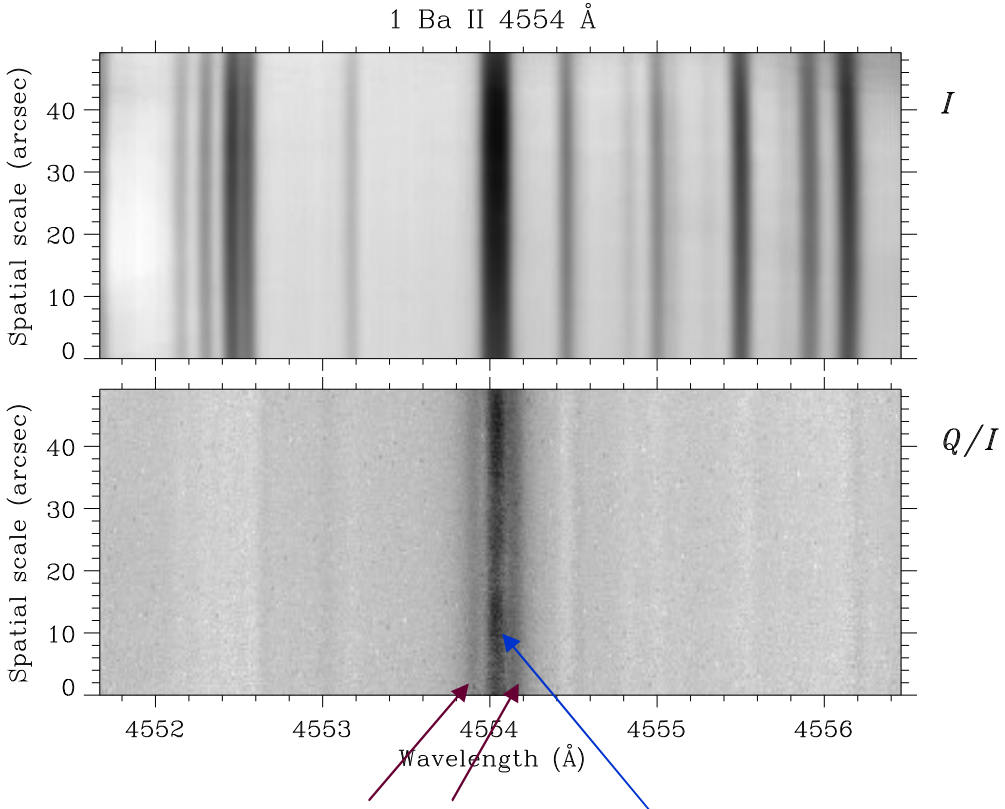

Hyperfine structure components due to the odd barium isotopes (with nuclear spin 3/2), which represent 18% of the Ba abundance

Central component due to the even isotopes (with zero nuclear spin)

Hyperfine splitting in scandium

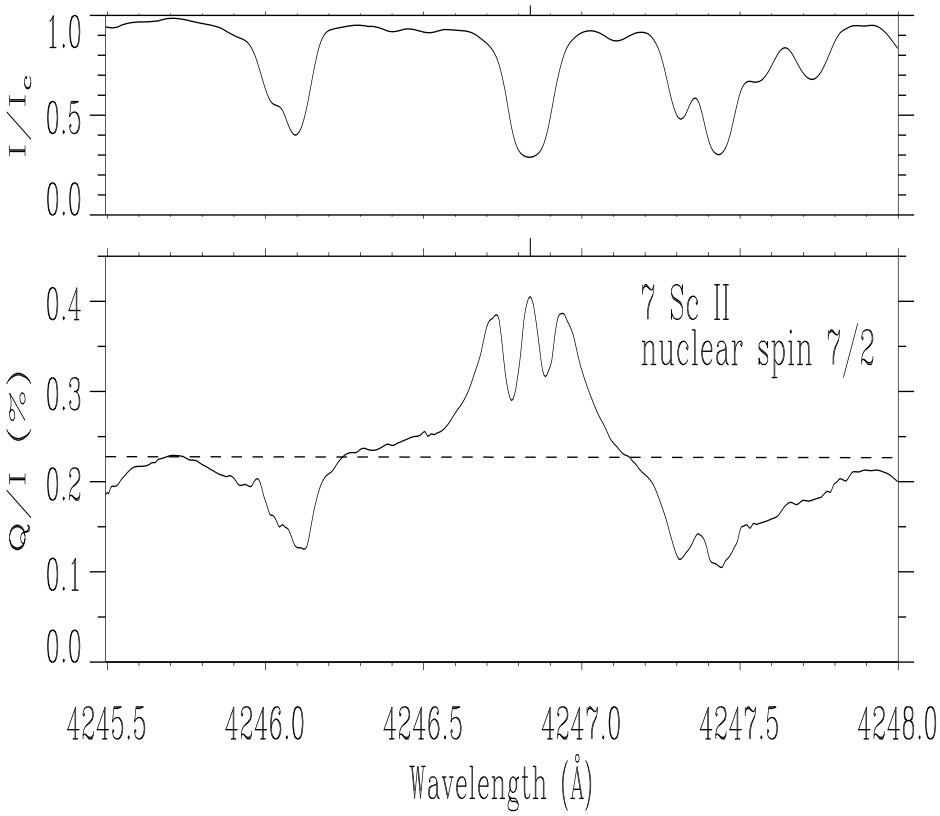

Institute of Astronomy ETH Zurich

Evidence for optical pumping that creates ground-state atomic polarization

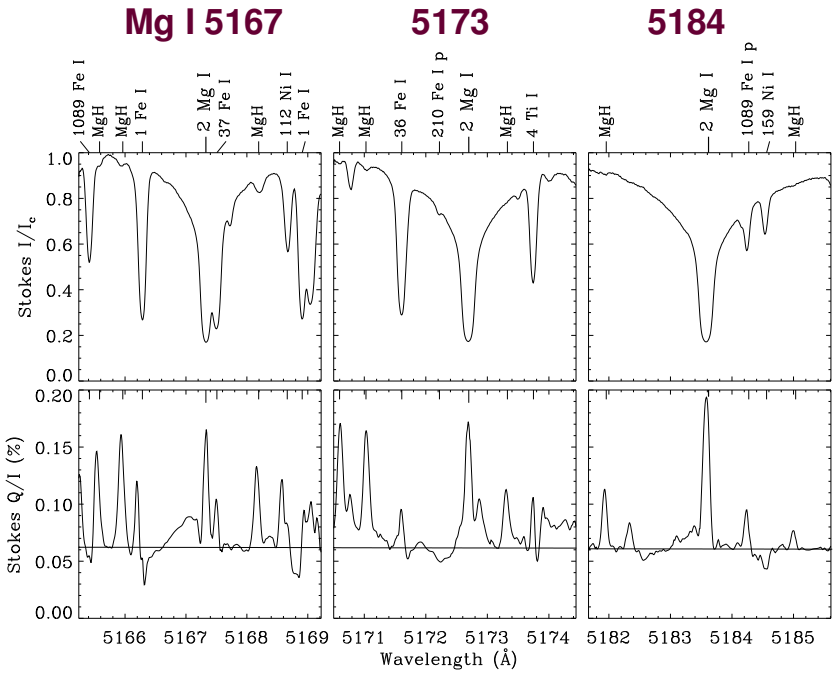

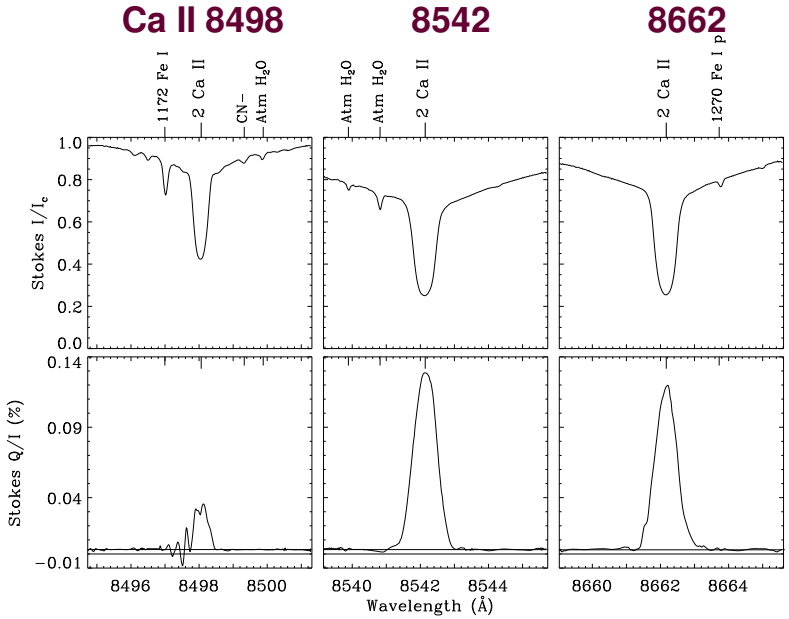

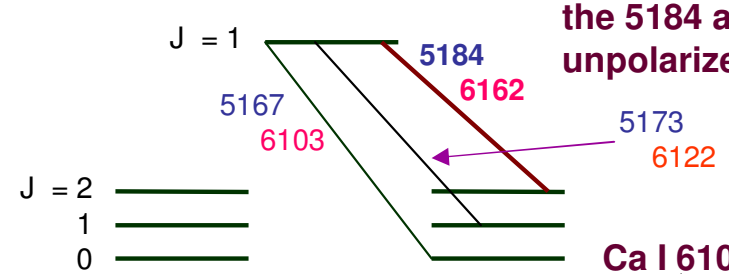

Without lower-level atomic polarization the 5184 and 6162 Å lines would be unpolarized

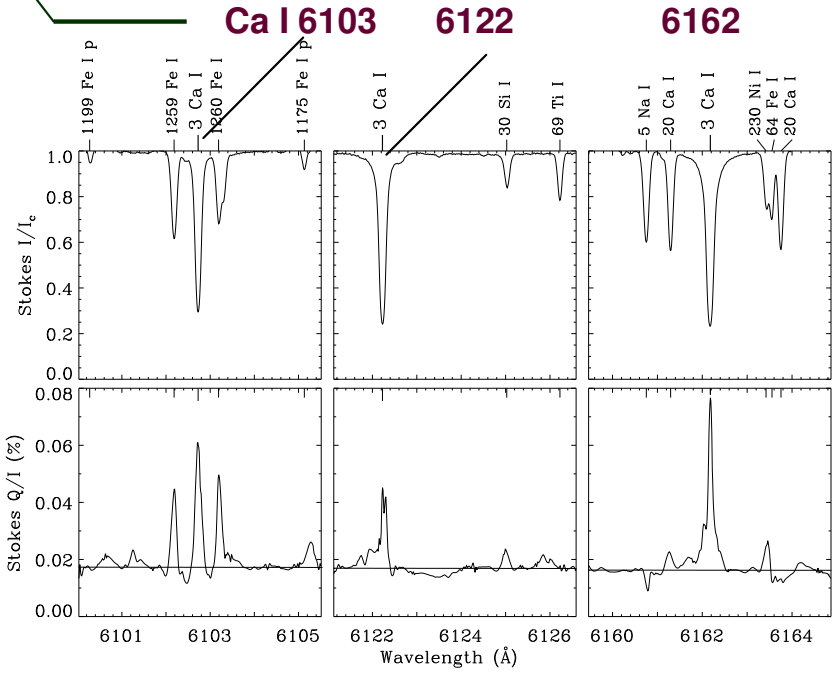

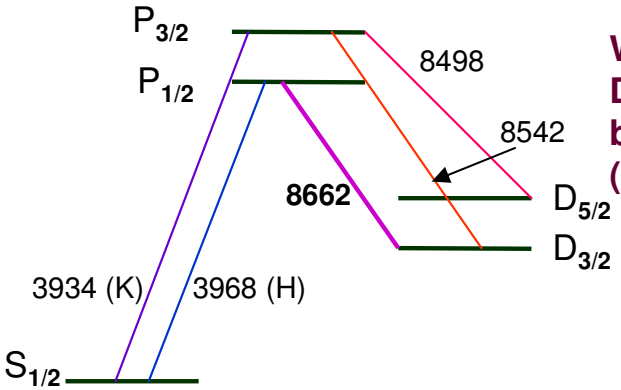

Without atomic polarization of the D levels the 8662 Å line would be unpolarized (Manso Sainz & Trujillo Bueno 2003)

Hanle depolarization by spatially unresolved turbulent magnetic fields

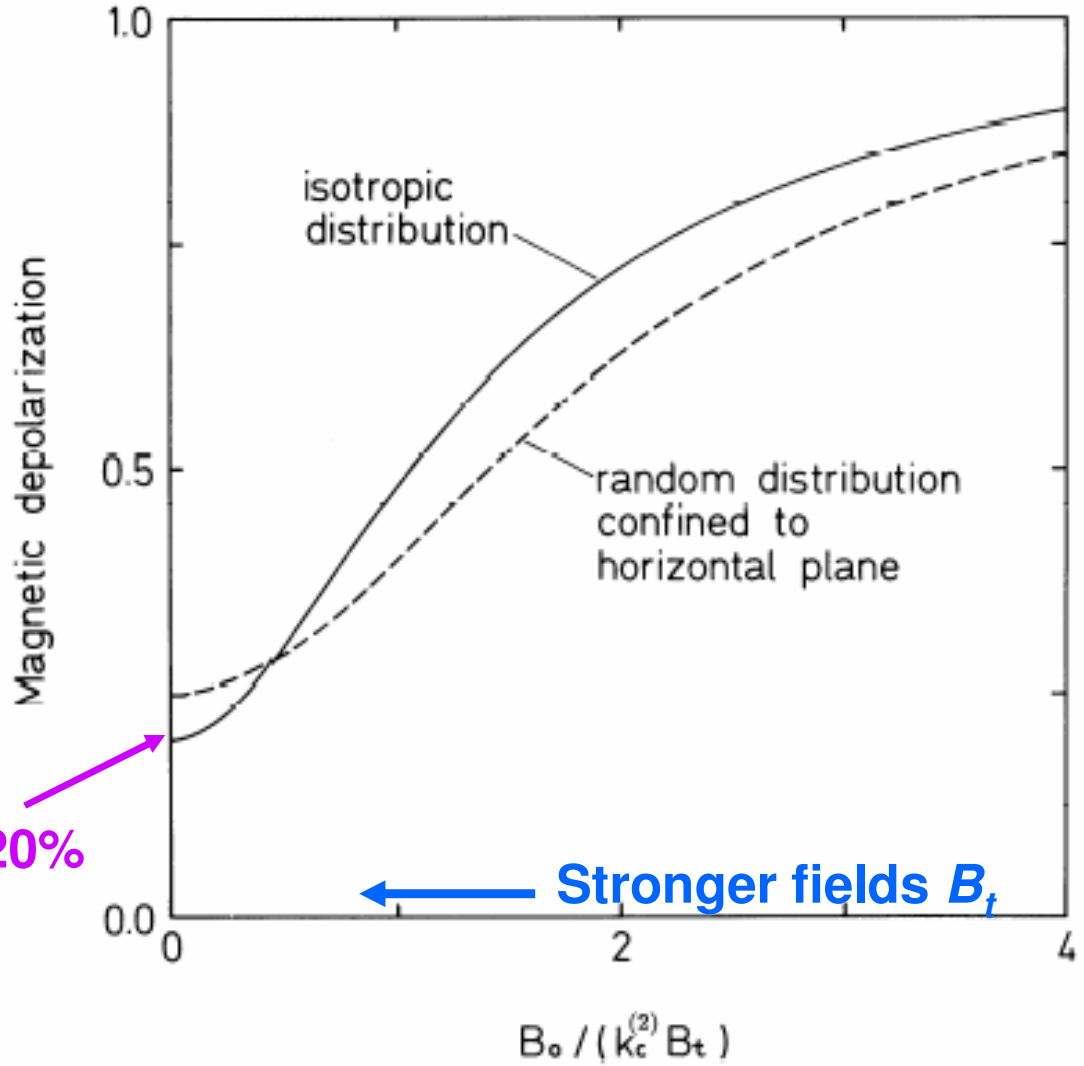

Saturation at 20%

Stronger fields B_t

Fig. 10.4. Magnetic depolarization $k_H^{(2)}$ vs. $B_0/(k_c^{(2)}B_t)$ for a turbulent field of strength B_t with an isotropic distribution of field vectors (solid line) and a randomly oriented field that is confined to the horizontal plane (dashed line). B_0 represents a field strength for which the Larmor precession rate equals the inverse radiative lifetime of the excited state. $k_c^{(2)}$ is the branching ratio representing the probability that the alignment of the excited state will not be destroyed during the scattering process. From Stenflo (1982).

Institute of Astronomy ETH Zurich

Hanle rotation in Sr I 4607 Å and Ba II 4554 Å, as observed with ZIMPOL on THEMIS